HHS Public Access

Author manuscript

J Comp Neurol. Author manuscript; available in PMC 2021 March 01.

Published in final edited form as:

J Comp Neurol. 2020 March 01; 528(4): 574–596. doi:10.1002/cne.24774.

Recurrent Laryngeal Nerve Transection in Mice Results in Translational Upper Airway Dysfunction

Megan M Haney[1], **Ali Hamad**[2], **Henok G Woldu**[3], **Michelle Ciucci**[4,5], **Nicole Nichols**[6], **Filiz Bunyak**[2], **Teresa E Lever**[6,7,*]

[1]Department of Veterinary Pathobiology, University of Missouri, Columbia, Missouri

[2]Department of Electrical Engineering and Computer Science, University of Missouri, Columbia, Missouri

[3]Department of Health Management & Informatics, University of Missouri, Columbia, Missouri

[4]Department of Communication Sciences and Disorders, University of Wisconsin–Madison, Madison, Wisconsin

[5]Department of Surgery, Division of Otolaryngology, University of Wisconsin-Madison, Madison, Wisconsin

[6]Department of Biomedical Sciences, University of Missouri, Columbia, Missouri

[7]Department of Otolaryngology–Head and Neck Surgery, University of Missouri, Columbia, Missouri

Abstract

The recurrent laryngeal nerve (RLN) is responsible for normal vocal fold (VF) movement, and is at risk for iatrogenic injury during anterior neck surgical procedures in human patients. Injury, resulting in VF paralysis, may contribute to subsequent swallowing, voice, and respiratory dysfunction. Unfortunately, treatment for RLN injury does little to restore physiologic function of the VFs. Thus, we sought to create a mouse model with translational functional outcomes to further investigate RLN regeneration and potential therapeutic interventions. To do so, we performed ventral neck surgery in 21 C57BL/6J male mice, divided into two groups: Unilateral RLN Transection (n=11) and Sham Injury (n=10). Mice underwent behavioral assays to determine upper airway function at multiple time points prior to and following surgery. Transoral endoscopy, videofluoroscopy, ultrasonic vocalizations, and whole-body plethysmography were used to assess VF motion, swallow function, vocal function, and respiratory function, respectively. Affected outcome metrics, such as VF motion correlation, intervocalization interval, and peak inspiratory flow were identified to increase the translational potential of this model. Additionally, immunohistochemistry was used to investigate neuronal cell death in the nucleus ambiguus. Results revealed that RLN transection created ipsilateral VF paralysis that did not recover by 13 weeks post-surgery. Furthermore, there was evidence of significant vocal and respiratory

[*]Corresponding Author: levert@health.missouri.edu; (573)-228-0723.

Conflicts of Interest

The authors declare that they have no conflict of interest.

Data Availability Statement: Research data are not shared.

dysfunction in the RLN transection group, but not the sham injury group. No significant differences in swallow function or neuronal cell death were found between the two groups. In conclusion, our mouse model of RLN injury provides several novel functional outcome measures to increase the translational potential of findings in preclinical animal studies. We will use this model and behavioral assays to assess various treatment options in future studies.

Graphical Abstract

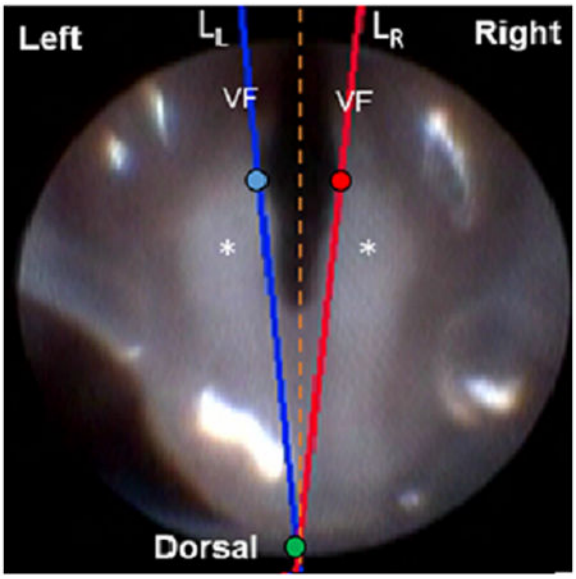

Keywords

Recurrent laryngeal nerve injury; unilateral vocal fold paralysis; animal model; dysphagia; dyspnea; dysphonia; RRID:AB_2532109; RRID:AB_141708

Introduction

Unilateral vocal fold (VF) paralysis is a common complication of iatrogenic recurrent laryngeal nerve (RLN) injury during cervical and thoracic surgeries. The incidence of RLN injury varies (~1-38%) depending on the surgical procedure performed (Beutler, Sweeney, & Connolly, 2001; Chandrasekhar et al., 2013; Daniero, Garrett, & Francis, 2014; Mattsson, Hydman, & Svensson, 2015). In patients with unilateral VF paralysis, 56% experience dysphagia, up to 80% are affected by dysphonia, and 75% encounter dyspnea (Brunner, Friedrich, Kiesler, Chibidziura-Priesching, & Gugatschka, 2011; Chandrasekhar et al., 2013; Choi et al., 2014). Moreover, dysphagia may result in life-threatening complications such as aspiration pneumonia, dehydration, and malnutrition (Anderson & Arnold, 2013), whereas dysphonia can greatly interfere with one's social life and employment, potentially necessitating a career change (Chandrasekhar et al., 2013). In fact, complications due to RLN palsy are among the leading reasons for litigation of healthcare professionals who perform these procedures (Aynehchi, McCoul, & Sundaram, 2010; Chandrasekhar et al., 2013; Choi et al., 2014; Ta, Liu, & Krishna, 2016).

Unfortunately, treatments that restore normal physiologic function after RLN injury are lacking (Chandrasekhar et al., 2013; Choi et al., 2014; Wang, Yuan, Xu, et al., 2016). Current strategies include voice therapy (Anderson & Arnold, 2013; Araki et al., 2006; Broniatowski et al., 2010; Neel et al., 1994) and medialization of the impaired VF (Anderson & Arnold, 2013). Alternative secondary surgeries, such as RLN anastomosis, may increase background muscle activity, but do not guarantee return of normal VF mobility (Choi et al., 2014). Thus, more effective neuro-regenerative treatment options are needed. However, to investigate new therapeutic interventions, a translational animal model that consistently replicates the functional outcomes of RLN injury in humans is essential. In addition, reliable functional assays to quantify these symptoms are critical.

Current models principally use transoral endoscopy to assess VF mobility and evaluate functional impairment and recovery after RLN injury (Hernandez-Morato, Sharma, & Pitman, 2016; Nishimoto, Kumai, & Yumoto, 2014; Tessema et al., 2009; Wang, Yuan, Chen, et al., 2016). While this methodology provides information on VF movement, it does not concurrently evaluate deficits associated with swallowing, vocalization, or respiration experienced by human patients. As these functions are fundamental to quality of life, it is essential to investigate them in animal models. However, no published study has comprehensively examined each potential complication in a single model.

An infant pig model of RLN injury has provided novel insights concerning the role of the RLN and its neural connections in swallowing behavior. By using videofluoroscopic techniques, RLN injury has been shown to result in compromised airway protection and esophageal dysphagia (Francois D. H. Gould et al., 2015), alterations in tongue shape (F. D. H. Gould, Yglesias, Ohlemacher, & German, 2017), and modified tongue and epiglottis kinematics during swallowing (F. D. Gould et al., 2016). However, these experiments were performed in neonatal and pre-weanling animals, better representing infants with immature nervous systems. In contrast, many patients undergoing common anterior neck procedures, such as thyroidectomy, belong to an aged population (Chandrasekhar et al., 2013; Marawar et al., 2010). Thus, a more appropriately aged animal with a fully developed nervous system is necessary to evaluate RLN injury and its sequela in this target population.

Rodents are ideal as aging models, as they age quickly compared to larger animal models. However, it is important to note the differences in swallowing behavior between mice and humans. Mice primarily use a licking behavior to acquire liquids, whereas humans more commonly use a cup or straw. Moreover, the larynx is anatomically protected in the murine nasopharynx, largely preventing laryngeal penetration or aspiration of food material. Despite these differences, both species use the tongue, jaw, and other oral cavity structures to facilitate the oral (i.e., preparatory or transport stage) and pharyngeal stages of swallowing and are presumed to utilize common neural substrates (Lever, Brooks, et al., 2015; Sang & Goyal, 2001). In fact, videofluoroscopic swallow studies have been used to document dysphagia in rodent models of amyotrophic lateral sclerosis (Lever, Braun, et al., 2015; Osman et al., 2019) and presbyphagia (Lever, Brooks, et al., 2015). The affected swallow metrics identified in these studies suggest that the swallowing mechanism is sufficiently similar between the two species and can be used in future investigations examining the neurologic pathways responsible for swallow function.

Of the post-operative complications associated with RLN injury, dysphonia is often the most problematic for the patient. One group assessed audible vocalizations in a rat model after RLN transection and showed hoarse, deep-pitched, and shorter vocalizations with low amplitudes (Wang, Yuan, Chen, et al., 2016; Wang, Yuan, Xu, et al., 2016). However, audible vocalizations are not the primary means of rodent communication and are elicited in response to stressful or painful stimuli, whereas ultrasonic vocalizations represent communicative intent (Lahvis, Alleva, & Scattoni, 2011). Furthermore, rodent ultrasonic vocalization assays have been well established (Blanchard, Agullana, McGee, Weiss, & Blanchard, 1992; Portfors, 2007; White, Prasad, Barfield, & Nyby, 1998). Though the exact physical mechanisms used to produce ultrasonic vocalizations remain to be elucidated (Mahrt, Agarwal, Perkel, Portfors, & Elemans, 2016), social ultrasonic vocalizations are analogous to human vocal communication in many important ways. For example, ultrasonic vocalizations are generated within the larynx (Roberts, 1975), are controlled by combinations of laryngeal anatomy, respiration, and laryngeal movement (Mahrt et al., 2016), and have symbolic reference that is capable of change in the behavior of the signal recipient (Brudzynski, 2005; Brudzynski & Pniak, 2002; Wohr, Houx, Schwarting, & Spruijt, 2008). As such, ultrasonic, rather than audible, vocalizations are a more appropriate method to study vocal function in rodents.

Similarly, comparative respiratory function has not been thoroughly assessed in animal models of RLN injury, except in coordination with swallowing in infant pigs (Ballester et al., 2018). Dyspnea after RLN injury is also under-researched in the human literature, likely because many human patients with unilateral VF paralysis have normal or near normal working respiratory capacity. However, up to ~75% complain of breathing impairment, especially during phonation or physical effort (Brunner et al., 2011). Of the few studies investigating respiratory parameters following RLN injury, most have noted decreased inspiratory flow rates in patients with unilateral VF paralysis, which may or may not be improved with VF medialization procedures (Asik et al., 2015; Kashima, 1984; Perie et al., 2002; Saarinen, Rihkanen, Lehikoinen-Soderlund, & Sovijarvi, 2000).

In this study, our general hypothesis was that RLN transection would significantly affect VF mobility, swallowing, vocalization, and respiration in an adult mouse model. We chose a transection injury as this is the most experimentally reproducible injury, and removes severity of injury as a confounding variable. Specifically, our hypotheses for each behavior were as follows:

H1) RLN transection would result in chronic ipsilateral VF paralysis;

H2) RLN transection would not result in aspiration (due to species differences in murine laryngeal anatomy), but would cause subtle deficits in swallowing behavior;

H3) RLN transection would decrease the number of ultrasonic vocalizations and impair acoustic parameters of these calls;

H4) RLN transection would impair respiration during respiratory challenge, but not during normal respiration.

H5) , In addition, RLN transection would not result in neuronal cell death in the ipsilateral brainstem nucleus, the nucleus ambiguus, due to the distal position of the lesion (Hydman, Svensson, Kuylenstierna, Ohlsson, & Mattsson, 2005; Mattsson et al., 2015).

Thus, we performed immunohistochemistry to investigate if neuronal cell death was present after RLN transection. We also continued to refine our VF tracking and quantification software (Hamad A, 2019; M. M. Haney, Hamad, Leary, Bunyak, & Lever, 2018) to better evaluate and characterize dynamic VF motion. Furthermore, behavioral tests were used to identify the most translational outcome measures for application towards human studies. Through this comprehensive behavioral regimen, this study offers the first look at the interplay between unilateral VF paralysis with the consequent somatic manifestations of dysphagia, dysphonia, and dyspnea in a single animal model.

Materials and Methods

Animals:

Animal care was conducted in accordance with the Guide for the Care and Use of Laboratory Animals and all experimental procedures performed in this study were reviewed and approved by the Institutional Animal Care and Use Committee at the University of Missouri, which is USDA-licensed and AAALAC-accredited. Twenty-one male C57BL/6J (B6) mice (age at beginning of study = 7.5 ± 0.6 months; weight = 30.4 ± 2.4 g) were used for this study. Mice were housed in individually ventilated caging (Tecniplast, West Chester, PA) with aspen chip bedding. Mice were group-housed (2-4 mice per cage) whenever possible throughout the study, and had free access to food (Laboratory Rodent Diet 5001, Purina, St. Louis, MO) and water, except for overnight water restriction for swallow assays, described below. Room temperature was maintained between 20.0 °C and 26.0 °C, relative humidity was between 30% to 70%, and the photoperiod was a 12:12-h standard light:dark cycle (lights on at 7:00 am). Standard enrichment (nestlet), running wheels, and mouse huts were provided to all cages.

All mice were of the same health status and were housed in the same room throughout the study; however, surgical manipulations and behavioral assays were performed in separate rooms of the laboratory, located outside of the vivarium. At the time of the study, serology samples from colony sentinels were tested quarterly and were considered free of the following agents: mouse hepatitis virus, minute virus of mice, mouse parvovirus, Sendai virus, Theiler's murine encephalomyelitis virus, mouse rotavirus, *Mycoplasma pulmonis, Pasteurella pneumotropica, Salmonella* spp., mouse pneumonia virus, reovirus 3, lymphocytic choriomeningitis virus, Ectromelia, mouse adenovirus 1 and 2, K virus, and polyoma virus. Fecal PCR was used to detect pinworms in sentinel mice, whereas cage PCR (pooled swabs by room) was used to detect fur mites, neither of which were detected.

Experimental Design:

Mice were randomized to undergo survival surgery to create an RLN transection injury (n=11), or a sham surgery to visualize, but not injure, the RLN (n=10). Transoral laryngoscopy was performed during surgery immediately prior to incision and immediately

after surgery to assess the effect on VF motion. In addition, mice underwent baseline behavioral testing prior to surgery to quantify normal swallow, vocal, and respiratory function. Testing consisted of videofluoroscopic swallow study, whole-body plethysmography, and ultrasonic vocalization assays. Mice received subsequent behavioral testing at various time points following surgical manipulations (Figure 1 and Table 1). At 13 weeks post-surgery (WPS), mice were anesthetized to repeat transoral laryngoscopy prior to euthanasia for tissue collection.

Surgical Procedures:

Mice were anesthetized with ketamine (90 mg/kg; Henry Schein, Melville, NY) and xylazine (11.25 mg/kg; Akorn, Lake Forest, IL), administered subcutaneously (SQ). Half doses of SQ ketamine were given to maintain the surgical plane of anesthesia every 10-20 min, as needed, throughout the procedure. The eyes were lubricated to prevent drying and the ventral neck was shaved and prepared aseptically for surgery. Mice were positioned in dorsal recumbency on a heated, custom platform beneath a surgical microscope (M125; Leica Microsystems, Inc., Buffalo Grove, IL), and reflexes (toe-pinch) were checked at least every 10-15 minutes.

A midline neck incision was made from the suprasternal notch to the mandible. The salivary glands were gently retracted laterally to expose the strap muscles overlying the trachea. In mice undergoing an RLN transection injury, the right RLN was isolated at the level of the 5th tracheal ring (Figure 2) and a small section of nerve (~1-2 mm) was removed to prevent RLN regeneration. The left RLN served as an internal control for this study. Mice in the sham injury group underwent an identical surgical procedure; however, the RLN was only visualized, not isolated or transected.

For both groups, the neck incision was closed with absorbable sutures (6-0 Monocryl, Ethicon, Somerville, NJ) and surgical glue (Tissumend II, Veterinary Products Laboratories; Phoenix, AZ). After suturing was complete, 0.2 ml of warm, sterile saline was administered SQ, along with buprenorphine-SR (1 mg/kg, SQ; Zoopharm, Windsor, CO), flunixin meglumine (2.2 mg/kg, SQ; Merck, Kenilworth, NJ), and atipamezole (0.22 mg/kg, SQ; Zoetis, Parsippany-Troy Hills, NJ) as separate injections for pain control and to reverse anesthesia. Mice were transferred to a clean, heated cage for recovery, and were monitored at least every 10-15 minutes until they were returned to their home cage once fully ambulatory. The home cages were placed half-on/half-off a heated water blanket (Model: TP700, Stryker, Kalamazoo, MI) overnight and returned to the vivarium the following morning. All mice were monitored daily for 1 week after surgery for any signs of pain, distress, or surgical complications.

Transoral Laryngoscopy (H1):

Transoral laryngoscopy was used to visualize VF movement (hypothesis 1). While mice were anesthetized for surgery, transoral laryngoscopy (M. M. Haney et al., 2018; Shock et al., 2015) was performed immediately prior to surgical incision to establish baseline VF movement and immediately after surgical manipulation to determine the direct effect on VF mobility. To do so, a micromanipulator-controlled sialendoscope (R11573A; Karl Storz,

Tuttlingen, Germany) with a customized laryngoscope was inserted into the oral cavity to visualize VF movement on a Storz Tele Pack X monitor (Karl Storz, Tuttlingen, Germany). In mice, VF movement is spontaneous with breathing, rather than an evoked response; therefore, no exogenous stimulus was required to elicit VF movement. Laryngoscopy was performed once more at 13 WPS with mice under anesthesia prior to euthanasia and tissue collection. Laryngoscopy videos were recorded at 30 frames per second (fps) for approximately 1-3 minutes per mouse for analysis.

Automated Vocal Fold Motion Analysis (H1):

Ten second clips from each laryngoscopy video were analyzed to detect left and right VF movement (for hypothesis 1) using our automated motion tracking software, VFTrack (M. M. Haney et al., 2018), and outcome metrics were calculated using our custom VFQuantify software (M. M. Haney et al., 2018). Briefly, points (p_L and p_R) were manually placed on the medial aspect of each VF or arytenoid cartilage on the first frame of each video clip. A third point (po), was placed midline, dorsal to the arytenoid cartilages. Separate lines (L_L and L_R) were automatically drawn from p_L and p_R to p_o to approximate the medial edge of each VF and its associated cartilage (Figure 3a). The VFs were automatically tracked using points on L_L and L_R at the same fixed distance from p_o. Left and right VF motion ranges and corresponding motion midlines (d_L=0 and d_R=0) were automatically computed based on displacement (in pixels) of the VFs. VF motion was graphically displayed as a cyclic waveform due to the oscillatory motion of the VFs during spontaneous breathing.

In addition to our previously published dynamic VF outcome metrics, Mean Motion Range Ratio and Open Close Cycle Ratio (M. M. Haney et al., 2018), we developed two additional metrics to characterize paradoxical movement of the right VF and compensation of the left VF, which we have observed in numerous mice after RLN injury. Abnormal, paradoxical movement of the VFs is characterized by the motion of the left and right VFs in the same direction, in contrast to the motion of the left and right VFs in the opposite direction during normal VF opening and closing behavior (Figure 3b). To differentiate between normal versus paradoxical movement, we have computed the motion correlation coefficient (Mcorr) (Kendall, 1979) between the time series of the left and right VF displacements. Mcorr is defined as,

$$Mcorr(d_L, d_R) = \frac{1}{N-1}\sum_{i=1}^{N}\left(\frac{\overline{d_L - \mu_L}}{\sigma_L}\right)\left(\frac{d_R - \mu_R}{\sigma_R}\right)$$

where d_L and d_R are displacements of the left and right VFs, and μ, σ denote mean and standard deviation of the displacement time series. The values of the correlation coefficients can range from −1 to 1, where values close to −1 represent a negative correlation (i.e., motion in opposite directions; normal function), values close to 1 represent a positive Mcorr (i.e., motion in the same direction; paradoxical VF motion), and values close to 0 represent minimal correlation. Based on the Mcorr values between the left and right VF displacement series, we have defined a VF motion activity index (VFActivity) as follows:

$$VF\ Activity = \begin{cases} -1 \le Mcorr\left(d_L, d_R\right) \le -0.5 & \text{Normal VF motion behavior} \\ -0.5 < Mcorr\left(d_L, d_R\right) < 0.5 & \text{Minimal motion correlation} \\ 0.5 \le Mcorr\left(d_L, d_R\right) \le 1 & \text{Paradoxical VF motion behavior (Pull or push)} \end{cases}$$

For the cases of paradoxical motion (VFActivity=Push/Pull), where the left and right VFs were moving in the same direction, further signal analysis was performed to differentiate pushing versus pulling behaviors. Pushing is characterized as the intact left VF pushing the injured right VF during glottal closing (adduction); while pulling is characterized as the intact VF pulling the injured VF during glottal opening (abduction) (Figure 4). Paradoxical motion is automatically classified as pushing versus pulling using the following processing steps:

1. In this model, the intact left VF moves symmetrically; therefore, its motion midline, $d_L=0$, is set as the steady state position for the left VF.
2. Left VF steady state crossing times (t_i) are detected as $d_L(t_i)=0$ (black dashed lines in Figure 5a).
3. Next, the steady state positions of the right, injured VF are determined as positions of the right VF when the left VF is positioned at its steady state (no pulling or pushing behavior by the left VF; dashed yellow lines in Figure 5a).
4. Pulling versus pushing behaviors are identified by separately computing total displacements of the right VF during positive and negative displacements of the left VF. Positive displacement of the left VF occurs when the left VF moves to the right of its motion midline ($d_L=0$) during adduction, indicated by positive movement on the displacement plots. Negative displacement of the left VF occurs when the left VF moves to the left of its motion midline ($d_L=0$), indicated by negative movement on the displacement plots. Larger total absolute displacement by the right VF during positive displacements of the left VF indicates pushing behavior (i.e., the area between the right VF and its steady state during positive displacements is greater than during negative displacements; Figure 5b). Larger total absolute displacement by the right VF during negative displacements of the left VF indicates pulling behavior (i.e., the area between the right VF and its steady state during negative displacements is greater than during positive displacements; Figure 5c).

Videofluoroscopic Swallow Study (H2):

For our second hypothesis, to assess swallowing function in awake, freely behaving mice, videofluoroscopic swallow testing was performed using our standard protocol (Lever, Braun, et al., 2015; Lever, Brooks, et al., 2015) at 4 time points: baseline (3 weeks prior to surgery), as well as 4 days post-surgery, 6 WPS, and 12 WPS. Videofluoroscopy was performed the week after whole-body plethysmography and ultrasonic vocalization assays to reduce the amount of testing for a single mouse in a given week. Four days post-surgery was chosen as

it was the earliest time point that mice could undergo fluoroscopy without risking confounding effects of post-surgical analgesics.

Prior to baseline swallow testing, mice underwent a behavioral conditioning program to assure familiarity and acceptance of the contrast solution and test chamber. For each time point, mice were fluid restricted overnight for 14-16 hours and provided additional chewable enrichment (e.g., nut and seed mix) to motivate voluntary drinking during testing. During testing, mice were individually enclosed in a custom test chamber positioned on a custom, remote-controlled lift table within a miniaturized fluoroscope (Glenbrook Technologies, Randolph, NJ). Each mouse was then exposed to approximately 2-3 minutes of low-dose radiation (~30 kV and 0.2 mA) for fluoroscopic examination of swallowing in the lateral plane while freely drinking a species-specific oral contrast agent recipe: Omnipaque (350 mg iodine per mL; GE Healthcare, Inc., Princeton, NJ) diluted to a 25% solution with deionized water and 3% chocolate syrup. The contrast solution was administered through a custom delivery system into a custom bowl positioned immediately above the test chamber floor.

To minimize radiation exposure, the fluoroscope was activated and video (30 fps) was recorded only when mice were drinking from the bowl, which was identified by real-time viewing via a webcam (C920 HD Pro Webcam; Logitech International S.A., Lausanne, Switzerland) positioned above the test chamber. Each video (AVI file) was subsequently analyzed frame-by-frame by two independent reviewers using video editing software (Pinnacle Studio 14; Corel Corporation, Ottawa, Ontario, Canada) to quantify several swallow metrics established by our prior work (Lever, Braun, et al., 2015; Lever, Brooks, et al., 2015). Metrics included lick rate (licks/second), swallow rate (swallows/2 seconds), inter-swallow interval (seconds), lick-swallow ratio (licks/swallow), pharyngeal transit time (seconds), esophageal transit time (seconds), and percentage of esophageal swallow inhibition (%). Each of these metrics was obtained from 3-5 two second clips of uninterrupted drinking. Reviewer discrepancies were resolved by group consensus.

Ultrasonic Vocalizations (H3):

An ultrasonic vocalization assay was used to assess our third hypothesis. As vocal function has been noted to recover shortly after RLN denervation (Nunez, Pomerantz, Bean, & Youngstrom, 1985), two acute time points and one chronic time point were selected to assess this functional outcome. Ultrasonic vocalization testing was performed to assess vocal function in mice 1 week prior to surgery and at 1, 2, and 5 WPS. Two to three nights prior to vocalization testing, mice were co-housed with a sexually mature female mouse overnight to sexually experience the male mice, as sexually experienced male mice are likely to produce greater numbers of ultrasonic calls (Chabout, Jones-Macopson, & Jarvis, 2017). For study feasibility, estrus cycle of the female mouse was not taken into account. The night prior to testing, male mice were individually housed in a clean cage to establish a home cage environment for data collection the following day. For testing, the entire home cage was placed in a custom sound insulated chamber. To elicit calls, a random female “intruder” mouse was anesthetized using ketamine and xylazine (90:11.25 mg/kg; SQ) and placed inside the home cage with the test subject (Hammerschmidt, Radyushkin, Ehrenreich, &

Fischer, 2012). This ensured that male-only vocalizations were obtained. The same intruder mouse was used approximately 4-6 times in succession until anesthetic depth began to lighten. Vocalization recording of the male mouse commenced immediately after placing the anesthetized female mouse in the test cage.

Individual vocalizations from the mice were recorded for 3 minutes using an ultrasonic microphone (CM16, Avisoft, Germany) with 16-bit resolution and a sampling rate of 250-kHz, placed directly over the test cage fitted with a modified wire bar lid (L. M. Grant et al., 2015; Laura M. Grant et al., 2014; Hammerschmidt et al., 2012). Offline acoustic analysis of vocal recordings for each mouse were analyzed using SASLab Pro (Avisoft, Germany). The WAV files were analyzed with Avisoft-generated spectrograms using a Fast Fourier Transform (FFT) of 512 points, frame size of 100%, flat top window, and temporal resolution set to display 75% overlap. A high pass filter was used to eliminate noise below 25 kHz (Laura M. Grant et al., 2014; Kelm-Nelson et al., 2018). The number of calls was automatically calculated by the Avisoft software and classified as low or high frequency modulated calls for all 4 time points. High frequency modulated calls were defined in the software as any call with a standard deviation of >0.1 for peak frequency of the entire call, whereas low frequency modulated calls had a standard deviation of ≤0.1 for peak frequency. These data were used to select the time points for additional in-depth ultrasonic vocalization analysis consisting of call labeling and acoustic parameters, from which we could identify potential outcome metrics that could be used for future studies in this model.

Using the high frequency modulated call results, baseline and 1 WPS were chosen for additional in depth analysis as follows: a trained reviewer independently classified and quantified all calls in a blinded fashion within the first 90 seconds after the first detected call. Ten call types (i.e., constant, downsweep, upsweep, harmonic, multiple jumps, jump up, jump down, half cycle, full cycle, and two cycle) were identified and grouped accordingly into four call categories based on complexity: simple, complex, jump, and cycle (Figure 6) (Laura M. Grant et al., 2014; Kelm-Nelson et al., 2018). The following acoustic properties that are common in communication signals among various species, including mice and humans, were measured for each call type and category (Basken, Connor, & Ciucci, 2012): percentage of call type (%), bandwidth (kHz), peak frequency (kHz), duration (millisecond, ms), and duration of peak frequency (ms).

Furthermore, mice preferentially produce ultrasonic calls in a repetitive series, which display a regular temporal structure (Gregg A. Castellucci, Calbick, & McCormick, 2018; G. A. Castellucci, McGinley, & McCormick, 2016; Sirotin, Costa, & Laplagne, 2014). Thus, additional ultrasonic vocalization metrics were used to further characterize potential dysfunction in repetitive calling in this model. To do so, series of calls within the first 90 seconds after the first call were manually identified using spectrogram files with labeled calls. Series of calls were defined as a group of at least four calls spaced no more than 150 ms apart from one another (i.e., an intervocalization interval < 150 ms; Figure 7) (G. A. Castellucci et al., 2016). The time in between series of calls was labeled as a pause. The number of call series and the average number of calls within a series, as well as the average length of call series and longest length of call series were calculated. In addition, the average intervocalization interval within a series was determined. Groups of less than four calls or

individual calls were counted as isolated calls within a pause. The average pause length and the average number of isolated calls within a pause were also calculated and compared between groups.

Whole-Body Plethysmography (H4):

Mice underwent baseline whole-body plethysmography within 3 weeks prior to surgery and at 1, 5 and 11 WPS to assess respiratory function for our fourth hypothesis. Unrestrained and unanesthetized mice were placed in individual plethysmography chambers (Data Sciences International, St. Paul, Minnesota) and exposed to normoxia (21% O_2) for 30 minutes to allow for unchallenged respiratory assessment. Mice were placed in the same chambers from week to week. Following normoxia, mice underwent a five minute hypercapnia (7% CO_2) and hypoxia (10.5% O_2) challenge (Lovett-Barr et al., 2012; Nichols, Gowing, et al., 2013; Nichols, Punzo, Duncan, Mitchell, & Johnson, 2013). As human patients complain of dyspnea with phonation or exercise, this hypercapnic/hypoxic challenge was utilized to obtain respiratory metrics in mice with increased respiratory effort to better correlate with human experiences.

A pressure calibration signal, ambient pressures, and chamber pressures were utilized for automated calculation of breath-by-breath respiratory parameters using Buxco FinePointe Software (Data Sciences International, St. Paul, Minnesota) to determine respiratory frequency (breaths/min), tidal volume (ml), inspiratory and expiratory time (seconds), peak inspiratory flow (ml/second), and minute ventilation (ml/min) for each mouse during normoxia and during the hypercapnic/hypoxic challenge. In addition, the apnea detection function within FinePointe software was used to identify sighs (2x the average amplitude of the respiratory waveform) (Real et al., 2007; Yamauchi et al., 2008) and apneas. An apnea was defined as the absence of at least two inspirations (i.e., a pause in breathing 2x the average frequency) (Matrot et al., 2005; Moore et al., 2014; Stettner, Zanella, Hilaire, & Dutschmann, 2008; Stettner, Zanella, Huppke, et al., 2008; Yamauchi, Kimura, & Strohl, 2010). The automatically detected sighs and apneas were manually reviewed for each mouse to verify accuracy and were excluded if not identified correctly, for example, if two shallow breaths were detected as an apnea rather than two individual breaths. The software was also used to calculate the percentage of erratic breathing, which is defined by the software as any breathing that was not classified as a normal breath, sigh, apnea, or sniff (Data Sciences International).

Neuronal Brainstem Histology (H5):

Lastly, neuronal brainstem histology was performed to investigate if cell death occurred for our fifth hypothesis. To do so, mice were euthanized with an intraperitoneal overdose injection of pentobarbital solution following the final laryngoscopy procedure at 13 WPS, and were perfused with saline followed by 4% paraformaldehyde (PFA). Brainstems were collected from each mouse and post-fixed overnight in 4% PFA at 4 °C. They were then placed in 20% sucrose solution for 3 days, followed by 30% sucrose and stored at 4 °C. Samples were replaced with fresh 30% sucrose solution with 1% sodium azide every 4 weeks until sectioning. Brainstems were sectioned at 40 μm on a freezing-sliding microtome (Leica SM 2010R, Wetzlar, Germany). All sections were stored free-floating at −20 °C in

tissue antifreeze solution (30% ethylene glycol, 30% glycerol, and 40% 1xPBS) in well plates with every 6th section/well.

One to two wells (randomly selected; containing every 6th section of serial 40 μm brainstem sections) from sham (n=6) and RLN transected (n=7) mice underwent fluorescent immunohistochemistry to identify and count neurons in the left and right nucleus ambiguus, the motor nucleus for the RLN (Yuan & Silberstein, 2016). After washing with 1X PBS and placing in a blocking solution with 5% normal donkey serum (NDS) for 1 hour, sections were incubated overnight in primary antibody, rabbit anti-NeuN (1:500, Abcam, ab177487; RRID:AB_2532109), to stain neuronal cell bodies. The following day, sections were washed with 1X PBS and then incubated in secondary antibody, anti-rabbit Alexa Fluor 488-conjugated antibody (1:1000; Molecular Probes, #A21206; RRID:AB_141708), for 2 hours. Sections were washed a final time in 1X PBS and immediately mounted on positively-charged glass slides. Slides were mounted with Prolong Gold Antifade Mountant with DAPI (ThermoFisher Scientific, # P36931) and allowed to air dry for 1 day in the dark. Slides were stored at −20 °C until quantification of staining was performed using an epifluorescence microscope (Model #:DM4000 B LED; Leica Biosystems, Wetzlar, Germany). Two to four sections containing an easily identifiable left and right nucleus ambiguus were randomly selected for each mouse for quantification (Figure 8). Sections incubated without primary and secondary antibodies served as negative controls. Stereo Investigator software (MBF Bioscience, Williston, VT) was used to count all neurons with a visible nucleolus within the entire nucleus ambiguus of each randomly selected section.

Statistics:

For normally distributed data, two-way repeated measures ANOVAs with surgical group (sham vs. transection) and time point as factors were performed using SigmaPlot 14.0 (Systat Software, San Jose, CA). If significant differences were indicated, multiple comparisons were made using a Tukey post hoc test. To take into account for any inherent baseline variability among the mice, a mixed effects model with a random intercept and group as fixed effects term was fitted using SAS 9.4 (SAS Institute, Cary, NC). To assess if the mean difference between the two groups also differed by time, the group*time interaction term was included in each of the fitted models. Post hoc Mann-Whitney U Tests were used to determine significant differences between the two experimental groups at each time point.

Baseline values often differed between groups for ultrasonic vocalization acoustic parameters and call series data, likely due to the inherently high acoustic variability in ultrasonic vocalizations (Riede, 2011). Thus, we fitted a regression model (Regression Model: Post_Surgery = Bo + B1*Group + B2*BaselineMeasure) using the baseline measurements as a covariate and the post-surgery measures as outcomes using SAS 9.4 (SAS Institute, Cary, NC). In addition, a two-way ANOVA was used to detect significant differences in mean neuron counts between experimental groups and the left and right nucleus ambiguus in each brainstem section. Analysis was performed using SigmaPlot 14.0 (Systat Software, San Jose, CA). *P* values less than or equal to 0.05 were considered significant for all tests.

Results

Effects of denervation on vocal fold motion (H1):

As hypothesized, RLN transection significantly impaired VF motion compared to sham mice. All transected mice developed immediate right (ipsilateral) VF paralysis, which persisted at 13 WPS. As expected, a two-way repeated measures ANOVA revealed significant differences for the mean motion range ratio and open close cycle ratio (Figure 9a **and** b) between groups at both post-surgical time points ($F_{2,38}$ = 181.40, P = < 0.001 and $F_{2,38}$ = 2124.14, P = < 0.001, respectively; Tukey post hoc = P = < 0.001 at both time points), signifying a decreased range and frequency of motion of the injured VF after RLN transection. Upon subjective review of each video, paradoxical movement of the right VF was noted in a subset of videos at both time points. In these cases, the right VF was moving in the same direction as the left VF, rather than its physiological normal direction (i.e., opposite direction of the left VF). However, the nature of this paradoxical movement was different between the two time points. If this movement was noted during the time immediately post-injury, the left VF appeared to be pulling the right VF, likely due to loss of tension on the injured side. Interestingly, if paradoxical movement was noted at the 13 WPS time point, the left VF seemed to be pushing the right VF, rather than pulling, indicating potential compensation by the left VF.

This paradoxical movement of the right VF contributed to increased range and frequency ratio measures for these mice, making it appear as if the right VF had physiologic movement, despite lack of normal function. Thus, in cases with positively correlated Mcorr values, a “0” was assigned to the mean motion range ratio and the threshold for the open close cycle ratio was manually adjusted within our VFQuantify software to more accurately represent the range and frequency of true physiologic motion of the impaired VF. In addition, we developed two novel outcome metrics to better characterize and document this abnormal movement of the VFs. Our first metric, Mcorr, calculates the correlation of the movement of the left VF compared to the right VF. In normal cases, the VFs are moving in opposite directions and are negatively correlated. In contrast, in instances of visible pushing or pulling motion, the VFs are moving in the same direction and are positively correlated. The sham mice retained a highly negative Mcorr value throughout the study, indicating normal directionality of VF movement. However, the transection mice developed minimally correlative or highly positive correlations at the two post-surgical time points (Figure 9c), signifying unilateral paralysis with or without abnormal movement of the injured VF. Mann-Whitney Rank Sum Tests revealed significant differences in Mcorr between the sham and RLN transection groups immediately post-surgery (T_{19} = 55.00, P = < 0.001) and at 13 WPS (T_{19} = 55.00, P = < 0.001). Mice with high positive Mcorr values were then automatically assigned a pushing or pulling activity classification based on the left VF steady state motion, quantified in Figure 9d.

Effects of denervation on swallowing (H2):

Though we hypothesized that swallow function would be impaired by RLN transection, no significant differences were found between groups for any swallow outcomes (P > 0.05). Reviewer discrepancies resolved by group consensus consisted of less than 15% of all

metrics analyzed. Outcomes for each videofluoroscopic swallow study metric are displayed in Table 2. Interestingly, esophageal transit time was noticeably longer for RLN transected mice, whereas esophageal transit for sham mice was appreciably shorter at 4 days post-surgery (Figure 10). Although a mixed effects model revealed a Group*Time interaction for esophageal transit time ($F_{3,390} = 3.75$, $P = 0.011$), there were no significant differences between groups at 4 days post-surgery ($T_{19} = 84.00$, $P = 0.072$) nor the other time points. In addition and in accordance with our hypothesis, laryngeal penetration or aspiration (i.e., contrast entering the airways), which are the most common manifestations of dysphagia in human patients with RLN injury, were not identified in any mice in this study.

Effects of denervation on vocalization (H3):

The total number of calls as well as the percentage of high frequency modulated calls were automatically detected by Avisoft Software and quantified for each group at all 4 time points (baseline, 1, 2, and 5 WPS). We hypothesized that the total number of vocalizations would decrease after RLN transection. Unexpectedly, a two-way repeated measures ANOVA revealed no significant differences in the total number of calls between groups ($F_{3,57} = 1.038$, $P = 0.38$; Figure 11a). However, a significant group*time interaction existed for the percentage of high frequency modulated calls ($F_{3,35} = 3.64$, $P = 0.022$), indicating the mean change over time between the two groups was different for these unique calls. Tukey post-hoc analysis revealed a significant decrease in high frequency modulated calls in the transection group at 1 WPS ($P = 0.031$; Figure 11b), which corresponded with an increase in the percentage of low frequency modulated calls in this group.

When comparing the percentage of high frequency modulated calls across all time points, 1 WPS showed significant differences between groups. Therefore, this time point, in addition to baseline, was chosen for additional in depth acoustic analysis. The goal of this analysis was to identify potential outcome metrics that could be used for future studies using this model. We hypothesized that RLN transection would impair acoustic parameters of specific call types. As such, all calls within 90 seconds after the 1st detected call were manually classified by a trained reviewer. Baseline measures were taken into account as a covariate to determine statistical significance between the sham and transection groups at 1 WPS for the following acoustic parameters: percentage of call type (%), bandwidth (kHz), duration (ms), peak frequency (kHz), and duration of peak frequency (ms). Results are summarized in Table 3. In particular, bandwidth appeared to be the most affected acoustic parameter at 1 WPS, with 3 call types (upsweep, jump down, and half cycle), and 2 subsequent call categories (simple and cycle) significantly affected by RLN transection (Figure 12). Lastly, we compared a number of outcome metrics related to the repetitive calling nature observed in mice. Though most outcomes were not significantly different between groups, the mean intervocalization interval was significantly longer in the RLN transection group at 1 WPS ($F_{1,12} = 7.20$, $P = 0.02$), and denervated mice showed a trend towards an increased number of isolated calls within a pause ($F_{1,12} = 3.37$, $P = 0.091$). These results are summarized in Table 4.

Effects of denervation on respiration (H4):

Respiratory parameters under normoxic conditions and hypercapnic/hypoxic conditions were analyzed separately. We hypothesized that respiration would be impaired during respiratory challenge, but not during normal respiration. As expected, in normoxia, there were no significant differences in frequency, tidal volume, inspiratory time, expiratory time, peak inspiratory flow, or minute ventilation between groups at any time point (Table 5). However, during the hypercapnic/hypoxic challenge, transected mice displayed a significant decrease in tidal volume and minute ventilation at 11 WPS compared to sham mice (Tukey post hoc: $P = 0.029$ and 0.047, respectively; Figure 13a **and** b). In addition, RLN transected mice displayed a trend for decreased peak inspiratory flows after injury. While there was not a statistically significant interaction between group and time point ($F_{3,57} = 2.473$; $P = 0.071$) for peak inspiratory flow, a two-tailed t-test performed for each individual time point revealed a statistically significant difference between groups at 11 WPS ($T_{19} = 2.67$, $P = 0.015$; Figure 13c). All other respiratory parameters were not significantly different between groups during the hypercapnic/hypoxic challenge (Table 6).

During normoxia, results of the mixed effects model revealed a statistically significant difference in the mean number of apneas between the two groups ($F_{1,57} = 11.64$, $P = 0.0012$). The group by interaction term was significant, indicating the change in the mean number of apneas over time was different between the two groups ($F_{3,57} = 6.88$, $P = 0.0005$). Post hoc Mann-Whitney U Tests showed significant differences between the two groups at all three post-surgical time points ($P < 0.004$ each), but not baseline ($P = 0.769$). Results of the estimated mean number of apneas by group over time is depicted in *Figure 14a.* The mixed effects model also detected a statistically significant mean difference between group ($F_{1,57} = 9.30$; $P = 0.0035$) and time point ($F_{3,57} = 20.06$; $P < 0.0001$) for the duration of apneas. There was no group by time interaction noted ($F_{3,57} = 2.29$; $P = 0.0876$), though Mann-Whitney U Tests at each time point revealed a significant decrease in the duration of apneas at 1 and 5 WPS for transected mice ($P = 0.021$ and 0.033, respectively; Figure 14b). The mean percentage of erratic breathing (Figure 14c) was also statistically significant between the two groups ($F_{1,57} = 19.53$, $P < 0.001$). Mean percentage of erratic breathing was lower in RLN transected mice across the three post-surgical time points (Mann-Whitney U Tests: $P = 0.0006$, 0.0008, 0.0006, at 1 WPS, 5WPS, and 11 WPS, respectively). In all mice, the number of apneas detected moderately correlated with the percentage of erratic breathing when analyzed using a Pearson Correlation ($R = 0.511$, $P < 0.0001$; Figure 14d). No differences in sighs were detected between groups.

Effect of RLN transection on motor neuron counts in the nucleus ambiguus (H5):

Here, we hypothesized that neuronal cell death would not occur in the ipsilateral nucleus ambiguus after RLN injury. Each mouse had 2-4 brainstem sections with an easily identifiable left and right nucleus ambiguus for analysis, all within the same brainstem region. On average, sham mice contained 65 (sd = 15) and 70 (sd = 20) neurons in the left and right nucleus ambiguus per section, respectively. RLN denervated mice contained 68 (sd = 14) and 67 (sd = 12) neurons in the left and right nucleus ambiguus per section, respectively. A two-way ANOVA did not detect a significant difference between groups or the left and right neuron counts for each section ($F_1 = 0.50$, $P = 0.48$).

Discussion

In this study, we built upon our previous work (Allen J, 2016; Newberry CI, 2016) developing a mouse model of laryngeal nerve injury. We have created a translational model that mirrors many of the sequela associated with RLN injury in human patients, including VF immobility, as well as vocal and respiratory dysfunction. A combination of behavioral testing, including endoscopic (M. M. Haney et al., 2018) and fluoroscopic (Lever, Braun, et al., 2015) imaging assays, along with ultrasonic vocalization and whole-body plethysmography assays allowed exploration of a wide range of potential functional complications (i.e., unilateral VF paralysis, dysphagia, dysphonia, and dyspnea) associated with RLN injury within the same animal. Furthermore, we continued to refine objective quantification of dynamic VF motion, including characterization of compensatory mechanisms of the uninjured VF. This study further validates our automated VF tracking software (M. M. Haney et al., 2018), and provides novel metrics to elucidate the mechanics of altered VF motion following RLN damage and subsequent recovery patterns.

As expected, mice experienced immediate unilateral VF paralysis after RLN transection, demonstrated by a decrease in range and frequency of right VF motion. In addition, a subset of denervated mice displayed paradoxical VF motion immediately after injury and at 13 WPS; however, the abnormal movement differed between time points. In both cases, physiological functional movement of the right VF was absent. Consequently, right VF motion appeared passive, such that the intact left VF “pulled” the right VF in an aberrant direction during *abduction* immediately post-transection. In contrast, at 13 WPS, *over-adduction* of the left VF resulted in contact with the right VF, thus displaying a pushing motion. Paradoxical VF movement has been reported in previous animal studies where RLN reinnervation was induced by repairing the transected nerve (Nishimoto et al., 2014; Nomura et al., 2010). It is presumable that the thyroarytenoid (adductor) muscle received aberrant reinnervation from former abductor axons, causing abnormal contraction of the intrinsic laryngeal muscles (i.e., synkinesis). Therefore, the paradoxical movement in these studies was likely due to active, but inappropriate muscle contraction, rather than the passive motion generated by the unaffected VF as observed in our current study. In addition, over-adduction of the unaffected VF has been noted in humans with unilateral VF paralysis (Tanaka, Chijiwa, & Hirano, 1993; Yumoto, Oyamada, Nakano, Nakayama, & Yamashita, 2004), though its role in functional compensation in patients with unilateral VF paralysis needs further investigation.

In addition to dynamic VF analysis, we continued to investigate dysphagia in this model. Unlike the infant pig model, RLN transection in adult B6 mice had minimal impact on swallowing behavior, as noted in our previous work (Allen J, 2016; Newberry CI, 2016). This finding is likely due to the anatomical differences between the mouse and human larynx. Yet, while murine laryngeal anatomy limits the assessment of aspiration (Lever, Braun, et al., 2015; Lever, Brooks, et al., 2015), other outcome metrics, especially those related to esophageal dysphagia, may be affected by RLN injury in this model. As the RLN also provides innervation to the esophagus in addition to the intrinsic laryngeal muscles, the trend for increased esophageal transit time following RLN transection observed in this study is consistent with pharyngoesophageal dysfunction documented in other RLN injury models

(Fukushima et al., 2005; Francois D. H. Gould et al., 2015; Tsujimura et al., 2018) and human unilateral VF paralysis patients (Aneas, Ricz, Mello-Filho, & Dantas, 2010; Wilson, Pryde, White, Maher, & Maran, 1995). As such, future studies may benefit by utilizing a higher speed camera to better capture the start and end points of esophageal bolus transit or alternative methods, such as manometry, to accurately determine if significant pharyngeal or esophageal dysphagia exists in this small, fast-drinking species.

Next, the effect of RLN injury on murine vocal function was assessed with ultrasonic vocalization analysis. Previous laryngeal nerve transection studies have shown that unilateral RLN injury disrupts ultrasonic vocalizations in rodents (Nunez et al., 1985; Roberts, 1975; Thomas, Talalas, & Barfield, 1981). However, these studies were limited in the acoustic parameters collected and lacked extensive analysis that is more easily performed with current technology. Our study offers the first robust analysis of vocalization acoustics following RLN injury in mice. Surprisingly, the number of calls generated did not differ between groups at any time point. However, high frequency modulated calls were significantly impaired by RLN injury at 1 WPS. Similarly, RLN transection impaired the frequency bandwidth of many call types at 1 WPS. These findings suggest that mice with unilateral VF paralysis lose the ability to modulate the frequency in their calls, similar to human patients who experience impairment in their phonation frequency (i.e., pitch range) following injury (Junuzovic-Zunic, Ibrahimagic, Altumbabic, Umihanic, & Izic, 2017; Sridhara, Ashok, Raghunathan, & Mann, 2003; Xue, Mittal, Zheng, & Bielamowicz, 2010). Unilateral VF paralysis patients also demonstrate impaired maximum phonation times (Sridhara et al., 2003), which was observed in the current study as decreased call durations and durations of peak frequency in a collection of call types in RLN transected mice. In addition to acoustic parameters, we examined murine ultrasonic vocalization call series, as patients with unilateral VF paralysis often suffer from vocal fatigue (Francis, McKiever, Garrett, Jacobson, & Penson, 2014). Indeed, RLN transection resulted in an increased intervocalization interval, requiring more time from the end of one vocalization to the next. An increased intervocalization interval may indicate VF fatigue, requiring more time to rest the VFs in between calls. Moreover, the trend for an increased number of isolated calls within a pause after RLN transection may act as another indicator of fatigue. Thus, we have identified several translational outcome measures to further investigate vocal impairment and recovery in this model.

Interestingly, the percentage of high frequency modulated calls in RLN transected mice recovered by 5 WPS, despite chronic ipsilateral VF paralysis at 13 WPS. The recovery pattern is consistent with previous literature demonstrating the effects of rodent RLN denervation on ultrasonic vocalizations are short-term (Nunez et al., 1985; Thomas et al., 1981). This recovery of vocalization may be due to a compensatory ability of the intact VF to cross the glottal midline and approximate the paralyzed VF as seen in a subset of mice during our endoscopy analysis. However, this is in contrast to humans, where over-adduction of the intact VF has been shown to result in worse vocal function (Yumoto et al., 2004). Thus, further work is necessary to establish the true compensatory nature of the intact VF and the exact mechanism of spontaneous vocal recovery in unilateral VF paralysis.

Lastly, we investigated the direct effect of RLN injury on respiratory function. Under normoxic conditions, respiratory parameters did not differ between groups. This was expected, as the majority of patients with unilateral VF paralysis do not develop significant abnormalities in their respiratory capacity (Brunner et al., 2011). However, many patients do complain of breathing difficulty during increased respiratory effort, such as during conversation and physical activity (Francis et al., 2014). As such, denervated mice exposed to a hypercapnic/hypoxic challenge to maximally increase their respiratory effort developed significantly impaired inspiratory flow, tidal volume, and minute ventilation at 11 WPS. Consistent with previous literature, inspiratory flow rate is often the most compromised spirometric parameter in human patients with unilateral VF paralysis (Asik et al., 2015). This outcome may be due to an increasingly atrophied and weakened VF that becomes flaccid and drawn into the inspiratory airstream, causing the VF to collapse and partially obstruct the airway. The obstruction of inspiratory flow would in turn limit tidal volume and minute ventilation. However, future studies utilizing EMG and/or histological assessments of the laryngeal muscles are necessary to confirm a lack of muscle tone and flaccid paralysis to support this hypothesis.

Furthermore, patients with unilateral VF paralysis report the inability to hold their breath and have an impaired ability to perform a valsalva maneuver (Francis et al., 2014), congruent with dysfunctional laryngeal closure. Thus, for this study, B6 mice were chosen as they have a propensity for dysrhythmic breathing contributing to spontaneous apneas (i.e., pauses in breathing) during wakefulness (Stettner, Zanella, Hilaire, et al., 2008; Stettner, Zanella, Huppke, et al., 2008). As apneas in this strain of mice have been associated with active laryngeal closure (Stettner, Zanella, Huppke, et al., 2008), we hypothesized that ipsilateral VF paralysis induced by RLN injury would prevent laryngeal closure and inhibit the ability to generate and sustain apneic episodes. In this study, RLN transection significantly decreased the number and duration of apneas, which correlated with a decrease in erratic breathing. This “stabilized” breathing pattern may suggest a central compensatory mechanism to ensure adequate ventilation with a dysfunctional VF. However, this observation may simply be a mechanical consequence of the inability of the mice to actively close their larynx, leading to less spontaneous apneas and less variation in their breathing patterns. It is interesting to note that some of the mice in our study that were found to have left VF compensation (pushing motion seen with laryngoscopy) also generated the most apneas within the RLN transection group at 11 WPS. Though a small sample size precludes statistical analysis, future studies may investigate if the compensatory contact (i.e., laryngeal closure) from the left VF contributes to increased apneas. The correlation between VF compensation and apnea production may be a useful outcome metric to determine whether a stabilized breathing pattern following RLN injury is due to central neurologic processes versus an anatomical laryngeal closure mechanism.

In addition to our behavioral analysis, we performed immunohistochemistry of the nucleus ambiguus to investigate neuronal cell counts at 13 WPS. Peripheral nerve injury often results in various percentages of retrograde cell death due to disruption in axon continuity (Navarro, Vivo, & Valero-Cabre, 2007). As the nucleus ambiguus is the motor nucleus containing cell bodies for the RLN, cell death may have occurred in the right nucleus ambiguus of the transection group. However, cell counts did not significantly differ between left and right

sides nor between treatment groups, likely because post-lesion cell death depends on numerous variables, such as age, severity of injury, and proximity of the injury to the soma (Navarro et al., 2007). Though we utilized the severest injury type (i.e., transection), our adult mice with fully developed nervous systems are less susceptible to cell death than those with immature neurons (Lowrie, Lavalette, & Davies, 1994; Snider, Elliott, & Yan, 1992). Moreover, a distal injury, such as in our study, is often associated with no or limited cell death (Hydman et al., 2005; Mattsson et al., 2015). An important caveat to our immunohistochemical investigations is that we limited our analysis to the easily recognizable compact region of the nucleus ambiguus, as this portion could be identified and outlined for counting purposes using our staining protocol. This leaves a large portion of the nucleus ambiguous uninvestigated. This allowed us to be as consistent in our sample analysis as possible. However, future studies should include nerve tracing experiments to identify cell death in all regions of the nucleus ambiguus to truly determine if there is a difference in cell numbers between groups.

In conclusion, we have identified several translational outcome measures in our mouse model of RLN injury, which we aim to utilize to objectively assess injury and subsequent recovery after RLN injury of various injury types and with different therapeutic interventions in future studies. In fact, we have begun work in a more prevalent RLN crush injury model to investigate electrical nerve stimulation as a potential treatment option. In this work (M. M. Haney, Allen J, Deninger I, Ohlhausen D, Ballenger B, Robbins K, Lever T, 2017), we have had preliminary success utilizing intraoperative vagal nerve stimulation as a clinically relevant treatment, though larger scale studies are necessary to establish optimal stimulation parameters. Furthermore, it is necessary to characterize the effects of intraoperative vagal nerve stimulation on all relative outcomes associated with swallowing, voice, and breathing as identified by this study, to understand its true translational potential.

Acknowledgements

This study was funded in part by National Institutes of Health Grant support (NIH T32-5T32OD011126-39 and NIH K99/R00 HL119606) and by the University of Missouri Coulter Translational Partnership. We graciously acknowledge Ian Deninger and John Szot for their assistance with ultrasonic vocalization analysis, as well as Victoria Caywood for videofluoroscopic swallow study analysis. We would also like to acknowledge Amy Keilholz and Lori Lind for their assistance in brainstem sectioning and training in IHC and neuronal cell counting, respectively. Lastly, we would like to thank Kate Osman for her diligent care and management of the rodent colony for this study.

References

Allen J TA, Robbins KL, Deninger I, Flynn K, Caywood V, Lever TE. (2016). A surgical mouse model of iatrogenic laryngeal nerve injury. Otolaryngology - Head and Neck Surgery, 155(1), 89–98.

Anderson KK, & Arnold PM (2013). Oropharyngeal Dysphagia after anterior cervical spine surgery: a review. Global Spine J, 3(4), 273–286. doi:10.1055/s-0033-1354253 [PubMed: 24436882]

Aneas GCG, Ricz HMA, Mello-Filho FV, & Dantas RO (2010). Swallowing Evaluation in Patients With Unilateral Vocal Fold Immobility. Gastroenterology research, 3(6), 245–252. doi:10.4021/gr270w [PubMed: 27942304]

Araki K, Shiotani A, Watabe K, Saito K, Moro K, & Ogawa K (2006). Adenoviral GDNF gene transfer enhances neurofunctional recovery after recurrent laryngeal nerve injury. Gene Ther, 13(4), 296–303. doi:10.1038/sj.gt.3302665 [PubMed: 16251996]

Asik MB, Karasimav O, Birkent H, Merati AL, Gerek M, & Yildiz Y (2015). Airway and Respiration Parameters Improve Following Vocal Fold Medialization: A Prospective Study. Ann Otol Rhinol Laryngol, 124(12), 972–977. doi:10.1177/0003489415593558 [PubMed: 26121983]

Aynehchi BB, McCoul ED, & Sundaram K (2010). Systematic review of laryngeal reinnervation techniques. Otolaryngol Head Neck Surg, 143(6), 749–759. doi:10.1016/j.otohns.2010.09.031 [PubMed: 21109073]

Ballester A, Gould F, Bond L, Stricklen B, Ohlemacher J, Gross A, German R (2018). Maturation of the Coordination Between Respiration and Deglutition with and Without Recurrent Laryngeal Nerve Lesion in an Animal Model. Dysphagia. doi:10.1007/s00455-018-9881-z

Basken JN, Connor NP, & Ciucci MR (2012). Effect of aging on ultrasonic vocalizations and laryngeal sensorimotor neurons in rats. Exp Brain Res, 219(3), 351–361. doi:10.1007/s00221-012-3096-6 [PubMed: 22562586]

Beutler WJ, Sweeney CA, & Connolly PJ (2001). Recurrent laryngeal nerve injury with anterior cervical spine surgery risk with laterality of surgical approach. Spine (Phila Pa 1976), 26(12), 1337–1342. [PubMed: 11426148]

Blanchard RJ, Agullana R, McGee L, Weiss S, & Blanchard DC (1992). Sex differences in the incidence and sonographic characteristics of antipredator ultrasonic cries in the laboratory rat (Rattus norvegicus). J Comp Psychol, 106(3), 270–277. [PubMed: 1395496]

Broniatowski M, Moore NZ, Grundfest-Broniatowski S, Tucker HM, Lancaster E, Krival K, Tyler DJ (2010). Paced glottic closure for controlling aspiration pneumonia in patients with neurologic deficits of various causes. Ann Otol Rhinol Laryngol, 119(3), 141–149. [PubMed: 20392026]

Brudzynski SM (2005). Principles of rat communication: quantitative parameters of ultrasonic calls in rats. Behav Genet, 35(1), 85–92. doi:10.1007/s10519-004-0858-3 [PubMed: 15674535]

Brudzynski SM, & Pniak A (2002). Social contacts and production of 50-kHz short ultrasonic calls in adult rats. J Comp Psychol, 116(1), 73–82. [PubMed: 11926686]

Brunner E, Friedrich G, Kiesler K, Chibidziura-Priesching J, & Gugatschka M (2011). Subjective breathing impairment in unilateral vocal fold paralysis. Folia Phoniatr Logop, 63(3), 142–146. doi: 10.1159/000316320 [PubMed: 20938194]

Castellucci GA, Calbick D, & McCormick D (2018). The temporal organization of mouse ultrasonic vocalizations. PLoS One, 13(10), e0199929. doi:10.1371/journal.pone.0199929 [PubMed: 30376572]

Castellucci GA, McGinley MJ, & McCormick DA (2016). Knockout of Foxp2 disrupts vocal development in mice. Sci Rep, 6, 23305. doi:10.1038/srep23305 [PubMed: 26980647]

Chabout J, Jones-Macopson J, & Jarvis ED (2017). Eliciting and Analyzing Male Mouse Ultrasonic Vocalization (USV) Songs. Jove(123), e54137. doi:10.3791/54137

Chandrasekhar SS, Randolph GW, Seidman MD, Rosenfeld RM, Angelos P, Barkmeier-Kraemer J, . . . Neck S. (2013). Clinical practice guideline: improving voice outcomes after thyroid surgery. Otolaryngol Head Neck Surg, 148(6 Suppl), S1–37. doi:10.1177/0194599813487301

Choi JS, Oh SH, An HY, Kim YM, Lee JH, & Lim JY (2014). Functional regeneration of recurrent laryngeal nerve injury during thyroid surgery using an asymmetrically porous nerve guide conduit in an animal model. Thyroid, 24(1), 52–59. doi:10.1089/thy.2013.0338 [PubMed: 24015805]

Daniero JJ, Garrett CG, & Francis DO (2014). Framework Surgery for Treatment of Unilateral Vocal Fold Paralysis. Curr Otorhinolaryngol Rep, 2(2), 119–130. doi:10.1007/s40136-014-0044-y [PubMed: 24883239]

Francis DO, McKiever ME, Garrett CG, Jacobson B, & Penson DF (2014). Assessment of patient experience with unilateral vocal fold immobility: a preliminary study. J Voice, 28(5), 636–643. doi:10.1016/j.jvoice.2014.01.006 [PubMed: 24739444]

Fukushima S, Shingai T, Takahashi Y, Taguchi Y, Noda T, & Yamada Y (2005). Genesis of the decrement of intraluminal pressure in the UES during swallowing in rabbits. Brain Res, 1044(1), 122–126. doi:10.1016/j.brainres.2005.03.001 [PubMed: 15862797]

Gould FD, Ohlemacher J, Lammers AR, Gross A, Ballester A, Fraley L, & German RZ (2016). Central nervous system integration of sensorimotor signals in oral and pharyngeal structures: oropharyngeal kinematics response to recurrent laryngeal nerve lesion. J Appl Physiol (1985), 120(5), 495–502. doi:10.1152/japplphysiol.00946.2015 [PubMed: 26679618]

Gould FDH, Lammers AR, Ohlemacher J, Ballester A, Fraley L, Gross A, & German RZ (2015). The physiologic impact of unilateral recurrent laryngeal nerve (RLN) lesion on infant oropharyngeal and esophageal performance. Dysphagia, 30(6), 714–722. doi:10.1007/s00455-015-9648-8 [PubMed: 26285799]

Gould FDH, Yglesias B, Ohlemacher J, & German RZ (2017). Pre-pharyngeal Swallow Effects of Recurrent Laryngeal Nerve Lesion on Bolus Shape and Airway Protection in an Infant Pig Model. Dysphagia, 32(3), 362–373. doi:10.1007/s00455-016-9762-2 [PubMed: 27873091]

Grant LM, Kelm-Nelson CA, Hilby BL, Blue KV, Paul Rajamanickam ES, Pultorak JD, Ciucci MR (2015). Evidence for early and progressive ultrasonic vocalization and oromotor deficits in a PINK1 gene knockout rat model of Parkinson's disease. J Neurosci Res, 93(11), 1713–1727. doi: 10.1002/jnr.23625 [PubMed: 26234713]

Grant LM, Richter F, Miller JE, White SA, Fox CM, Zhu C, Ciucci MR (2014). Vocalization deficits in mice over-expressing alpha-synuclein, a model of pre-manifest Parkinson's disease. Behavioral neuroscience, 128(2), 110–121. doi:10.1037/a0035965 [PubMed: 24773432]

Hamad A HM, Lever TE, Bunyak F. (2019). Automated Segmentation of the Vocal Folds in Laryngeal Endoscopy Videos Using Deep Convolutional Regression Networks. Proceedings of the IEEE Conference on Computer Vision and Pattern Recognition Workshops.

Hammerschmidt K, Radyushkin K, Ehrenreich H, & Fischer J (2012). The structure and usage of female and male mouse ultrasonic vocalizations reveal only minor differences. PLoS One, 7(7), e41133. doi:10.1371/journal.pone.0041133 [PubMed: 22815941]

Haney MM, Allen J, Deninger I, Ohlhausen D, Ballenger B, Robbins K, Lever T. (2017). Dysphagia Research Society Annual Meeting March 2–4, 2017 : The Hilton Portland and Executive Tower, Portland, Oregon. Dysphagia, 32(6), 799–858. doi:10.1007/s00455-017-9805-3 [PubMed: 28470543]

Haney MM, Hamad A, Leary E, Bunyak F, & Lever TE (2018). Automated Quantification of Vocal Fold Motion in a Recurrent Laryngeal Nerve Injury Mouse Model. Laryngoscope. doi:10.1002/lary.27609

Hernandez-Morato I, Sharma S, & Pitman MJ (2016). Changes in neurotrophic factors of adult rat laryngeal muscles during nerve regeneration. Neuroscience, 333, 44–53. doi:10.1016/j.neuroscience.2016.07.004 [PubMed: 27421227]

Hydman J, Svensson M, Kuylenstierna R, Ohlsson M, & Mattsson P (2005). Neuronal survival and glial reactions after recurrent laryngeal nerve resection in the rat. Laryngoscope, 115(4), 619–624. doi:10.1097/01.mlg.0000161362.43320.b2 [PubMed: 15805870]

Junuzovic-Zunic L, Ibrahimagic A, Altumbabic S, Umihanic S, & Izic B (2017). Improving Voice Outcomes After Injury to the Recurrent Laryngeal Nerve (Vol. 15).

Kashima HK (1984). Documentation of upper airway obstruction in unilateral vocal cord paralysis: flow-volume loop studies in 43 subjects. Laryngoscope, 94(7), 923–937. [PubMed: 6738272]

Kelm-Nelson CA, Brauer AFL, Barth KJ, Lake JM, Sinnen MLK, Stehula FJ, Ciucci MR (2018). Characterization of early-onset motor deficits in the Pink1−/− mouse model of Parkinson disease. Brain Res, 1680, 1–12. doi:10.1016/j.brainres.2017.12.002 [PubMed: 29229503]

Kendall MG (1979). The Advanced Theory of Statistics (Vol 4th Ed): Macmillan.

Lahvis GP, Alleva E, & Scattoni ML (2011). Translating Mouse Vocalizations: Prosody and Frequency Modulationenes. Brain Behav, 10(1), 4–16. doi:10.1111/j.1601-183X.2010.00603.x

Lever TE, Braun SM, Brooks RT, Harris RA, Littrell LL, Neff RM, Ulsas MA (2015). Adapting human videofluoroscopic swallow study methods to detect and characterize dysphagia in murine disease models. J Vis Exp(97). doi:10.3791/52319

Lever TE, Brooks RT, Thombs LA, Littrell LL, Harris RA, Allen MJ, Robbins KL (2015). Videofluoroscopic Validation of a Translational Murine Model of Presbyphagia. Dysphagia, 30(3), 328–342. doi:10.1007/s00455-015-9604-7 [PubMed: 25783697]

Lovett-Barr MR, Satriotomo I, Muir GD, Wilkerson JE, Hoffman MS, Vinit S, & Mitchell GS (2012). Repetitive intermittent hypoxia induces respiratory and somatic motor recovery after chronic cervical spinal injury. J Neurosci, 32(11), 3591–3600. doi:10.1523/jneurosci.2908-11.2012 [PubMed: 22423083]

Lowrie MB, Lavalette D, & Davies CE (1994). Time Course of Motoneurone Death after Neonatal Sciatic Nerve Crush in the Rat. Developmental Neuroscience, 16(5–6), 279–284. doi: 10.1159/000112120 [PubMed: 7768206]

Mahrt E, Agarwal A, Perkel D, Portfors C, & Elemans CP (2016). Mice produce ultrasonic vocalizations by intra-laryngeal planar impinging jets. Curr Biol, 26(19), R880–r881. doi:10.1016/j.cub.2016.08.032 [PubMed: 27728788]

Marawar S, Girardi FP, Sama AA, Ma Y, Gaber-Baylis LK, Besculides MC, & Memtsoudis SG (2010). National trends in anterior cervical fusion procedures. Spine (Phila Pa 1976), 35(15), 1454–1459. doi:10.1097/BRS.0b013e3181bef3cb [PubMed: 20216341]

Matrot B, Durand E, Dauger S, Vardon G, Gaultier C, & Gallego J (2005). Automatic classification of activity and apneas using whole body plethysmography in newborn mice. J Appl Physiol (1985), 98(1), 365–370. doi:10.1152/japplphysiol.00803.2004 [PubMed: 15591306]

Mattsson P, Hydman J, & Svensson M (2015). Recovery of laryngeal function after intraoperative injury to the recurrent laryngeal nerve. GlandSurg, 4(1), 27–35. doi:10.3978/j.issn.2227-684X.2015.01.10

Moore MW, Akladious A, Hu Y, Azzam S, Feng P, & Strohl KP (2014). Effects of orexin 2 receptor activation on apnea in the C57BL/6J mouse. Respir Physiol Neurobiol, 200, 118–125. doi: 10.1016/j.resp.2014.03.014 [PubMed: 24929062]

Navarro X, Vivo M, & Valero-Cabre A. (2007). Neural plasticity after peripheral nerve injury and regeneration. Prog Neurobiol, 82(4), 163–201. doi:10.1016/j.pneurobio.2007.06.005 [PubMed: 17643733]

Neel HB, Harner SG, Benninger MS, Crumley RL, Ford CN, Gould WJ, Sataloff RT (1994). Evaluation and Treatment of the Unilateral Paralyzed Vocal Fold. Otolaryngology -- Head and Neck Surgery, 111(4), 497–508. doi:10.1177/019459989411100419 [PubMed: 7936686]

Newberry CI LT, Allen J, Thiessen A, Hopewell B. (2016). A surgical mouse model of iatrogenic laryngeal nerve injury. Dysphagia, 31, 786–845.

Nichols NL, Gowing G, Satriotomo I, Nashold LJ, Dale EA, Suzuki M, Mitchell GS (2013). Intermittent hypoxia and stem cell implants preserve breathing capacity in a rodent model of amyotrophic lateral sclerosis. Am J Respir Crit Care Med, 187(5), 535–542. doi:10.1164/rccm.201206-1072OC [PubMed: 23220913]

Nichols NL, Punzo AM, Duncan ID, Mitchell GS, & Johnson RA (2013). Cervical spinal demyelination with ethidium bromide impairs respiratory (phrenic) activity and forelimb motor behavior in rats. Neuroscience, 229, 77–87. doi:10.1016/j.neuroscience.2012.10.066 [PubMed: 23159317]

Nishimoto K, Kumai Y, & Yumoto E (2014). Paradoxical movement of rat vocal folds following recurrent laryngeal nerve injury. Acta Otolaryngol, 134(11), 1164–1171. doi: 10.3109/00016489.2014.936625 [PubMed: 25315916]

Nomura K, Kunibe I, Katada A, Wright CT, Huang S, Choksi Y, Zealear DL (2010). Bilateral motion restored to the paralyzed canine larynx with implantable stimulator. Laryngoscope, 120(12), 2399–2409. doi:10.1002/lary.21065 [PubMed: 21053243]

Nunez AA, Pomerantz SM, Bean NJ, & Youngstrom TG (1985). Effects of laryngeal denervation on ultrasound production and male sexual behavior in rodents. Physiol Behav, 34(6), 901–905. [PubMed: 4059379]

Osman KL, Kohlberg S, Mok A, Brooks R, Lind LA, McCormack K, Lever TE (2019). Optimizing the Translational Value of Mouse Models of ALS for Dysphagia Therapeutic Discovery. Dysphagia. doi:10.1007/s00455-019-10034-9

Perie S, Roubeau B, Liesenfelt I, Chaigneau-Debono G, Bruel M, & St Guily JL (2002). Role of medialization in the improvement of breath control in unilateral vocal fold paralysis. Ann Otol Rhinol Laryngol, 111(11), 1026–1033. doi:10.1177/000348940211101114 [PubMed: 12450179]

Portfors CV (2007). Types and functions of ultrasonic vocalizations in laboratory rats and mice. Journal of the American Association for Laboratory Animal Science, 46(1), 28–34. [PubMed: 17203913]

Real C, Popa D, Seif I, Callebert J, Launay J-M, Adrien J, & Escourrou P (2007). Sleep Apneas are Increased in Mice Lacking Monoamine Oxidase A. Sleep, 30(10), 1295–1302. [PubMed: 17969463]

Riede T (2011). Subglottal pressure, tracheal airflow, and intrinsic laryngeal muscle activity during rat ultrasound vocalization. J Neurophysiol, 106(5), 2580–2592. doi:10.1152/jn.00478.2011 [PubMed: 21832032]

Roberts LH (1975). Evidence for the laryngeal source of ultrasonic and audible cries of rodents. Journal of Zoology, 175(2), 243–257. doi:10.1111/j.1469-7998.1975.tb01399.x

Saarinen A, Rihkanen H, Lehikoinen-Soderlund S, & Sovijarvi AR (2000). Airway flow dynamics and voice acoustics after autologous fascia augmentation of paralyzed vocal fold. Ann Otol Rhinol Laryngol, 109(6), 563–567. doi:10.1177/000348940010900606 [PubMed: 10855567]

Sang Q, & Goyal RK (2001). Swallowing reflex and brain stem neurons activated by superior laryngeal nerve stimulation in the mouse. Am J Physiol Gastrointest Liver Physiol, 280(2), G191–200. doi:10.1152/ajpgi.2001.280.2.G191 [PubMed: 11208540]

Shock LA, Gallemore BC, Hinkel CJ, Szewczyk MM, Hopewell BL, Allen MJ, Lever TE (2015). Improving the Utility of Laryngeal Adductor Reflex Testing: A Translational Tale of Mice and Men. Otolaryngol Head Neck Surg, 153(1), 94–101. doi:10.1177/0194599815578103 [PubMed: 25832829]

Sirotin YB, Costa ME, & Laplagne DA (2014). Rodent ultrasonic vocalizations are bound to active sniffing behavior. Front Behav Neurosci, 8, 399. doi:10.3389/fnbeh.2014.00399 [PubMed: 25477796]

Snider WD, Elliott JL, & Yan Q (1992). Axotomy-induced neuronal death during development. Journal of Neurobiology, 23(9), 1231–1246. doi:doi:10.1002/neu.480230913 [PubMed: 1469386]

Sridhara SR, Ashok KG, Raghunathan M, & Mann SB (2003). To study voice quality before and after thyroplasty type 1 in patients with symptomatic unilateral vocal cord paralysis. Am J Otolaryngol, 24(6), 361–365. [PubMed: 14608566]

Stettner GM, Zanella S, Hilaire G, & Dutschmann M (2008). 8-OH-DPAT suppresses spontaneous central apneas in the C57BL/6J mouse strain. Respir Physiol Neurobiol, 161(1), 10–15. doi: 10.1016/j.resp.2007.11.001 [PubMed: 18155647]

Stettner GM, Zanella S, Huppke P, Gartner J, Hilaire G, & Dutschmann M (2008). Spontaneous central apneas occur in the C57BL/6J mouse strain. Respir Physiol Neurobiol, 160(1), 21–27. doi: 10.1016/j.resp.2007.07.011 [PubMed: 17869191]

Ta JH, Liu YF, & Krishna P (2016). Medicolegal Aspects of Iatrogenic Dysphonia and Recurrent Laryngeal Nerve Injury. Otolaryngol Head Neck Surg, 154(1), 80–86. doi: 10.1177/0194599815607220 [PubMed: 26419840]

Tanaka S, Chijiwa K, & Hirano M (1993). Study on Over-Adduction of Unaffected Vocal Fold in Unilateral Recurrent Laryngeal Nerve Paralysis (Vol 5).

Tessema B, Roark RM, Pitman MJ, Weissbrod P, Sharma S, & Schaefer SD (2009). Observations of recurrent laryngeal nerve injury and recovery using a rat model. Laryngoscope, 119(8), 1644–1651. doi:10.1002/lary.20293 [PubMed: 19504559]

Thomas DA, Talalas L, & Barfield RJ (1981). Effect of devocalization of the male on mating behavior in rats. Journal of Comparative and Physiological Psychology, 95(4), 630–637. doi:10.1037/h0077803

Tsujimura T, Suzuki T, Yoshihara M, Sakai S, Koshi N, Ashiga H, Inoue M (2018). Involvement of hypoglossal and recurrent laryngeal nerves on swallowing pressure. J Appl Physiol (1985), 124(5), 1148–1154. doi:10.1152/japplphysiol.00944.2017 [PubMed: 29357492]

Wang B, Yuan J, Chen X, Xu J, Li Y, & Dong P (2016). Functional regeneration of the transected recurrent laryngeal nerve using a collagen scaffold loaded with laminin and laminin-binding BDNF and GDNF. Sci Rep, 6, 32292. doi:10.1038/srep32292 [PubMed: 27558932]

Wang B, Yuan J, Xu J, Xie J, Wang G, & Dong P (2016). Neurotrophin expression and laryngeal muscle pathophysiology following recurrent laryngeal nerve transection. Mol Med Rep, 13(2), 1234–1242. doi:10.3892/mmr.2015.4684 [PubMed: 26677138]

White NR, Prasad M, Barfield RJ, & Nyby JG (1998). 40- and 70-kHz vocalizations of mice (Mus musculus) during copulation. Physiol Behav, 63(4), 467–473. [PubMed: 9523885]

Wilson JA, Pryde A, White A, Maher L, & Maran AG (1995). Swallowing performance in patients with vocal fold motion impairment. Dysphagia, 10(3), 149–154. [PubMed: 7614853]

Wohr M, Houx B, Schwarting RK, & Spruijt B (2008). Effects of experience and context on 50-kHz vocalizations in rats. Physiol Behav, 93(4–5), 766–776. doi:10.1016/j.physbeh.2007.11.031 [PubMed: 18191963]

Xue Q, Mittal R, Zheng X, & Bielamowicz S (2010). A computational study of the effect of vocal-fold asymmetry on phonation. J Acoust Soc Am, 128(2), 818–827. doi:10.1121/1.3458839 [PubMed: 20707451]

Yamauchi M, Kimura H, & Strohl KP (2010). Mouse models of apnea: strain differences in apnea expression and its pharmacologic and genetic modification. Adv Exp Med Biol, 669, 303–307. doi:10.1007/978-1-4419-5692-7_62 [PubMed: 20217371]

Yamauchi M, Ocak H, Dostal J, Jacono FJ, Loparo KA, & Strohl KP (2008). Post-sigh breathing behavior and spontaneous pauses in the C57BL/6J (B6) mouse. Respir Physiol Neurobiol, 162(2), 117–125. doi:10.1016/j.resp.2008.05.003 [PubMed: 18565803]

Yuan H, & Silberstein SD (2016). Vagus Nerve and Vagus Nerve Stimulation, a Comprehensive Review: Part I. Headache, 56(1), 71–78. doi:10.1111/head.12647 [PubMed: 26364692]

Yumoto E, Oyamada Y, Nakano K, Nakayama Y, & Yamashita Y (2004). Three-dimensional characteristics of the larynx with immobile vocal fold. Arch Otolaryngol Head Neck Surg, 130(8), 967–974. doi:10.1001/archotol.130.8.967 [PubMed: 15313868]

The recurrent laryngeal nerve (RLN) is responsible for vocal fold (VF) movement, and is at risk for iatrogenic injury during anterior neck surgical procedures in human patients. Injury, resulting in VF paralysis, may contribute to subsequent swallowing, voice, and respiratory dysfunction. Treatment does little to restore physiologic function of the VFs. Thus, we sought to create a mouse model with translational functional outcomes to investigate RLN regeneration and potential therapeutic interventions. We used our custom laryngoscopy equipment to visualize the VFs before and after RLN injury. In addition, we further refined our automated VF tracking and quantification software to quantify VF movement and potential recovery. In this study, we included additional behavioral tests including videofluoroscopy, ultrasonic vocalizations, and whole-body plethysmography to assess swallowing, vocalization, and respiration, respectively. Results generated from this study provide novel outcome metrics to characterize RLN injury in this mouse model and can be used to investigate treatment options in future studies.

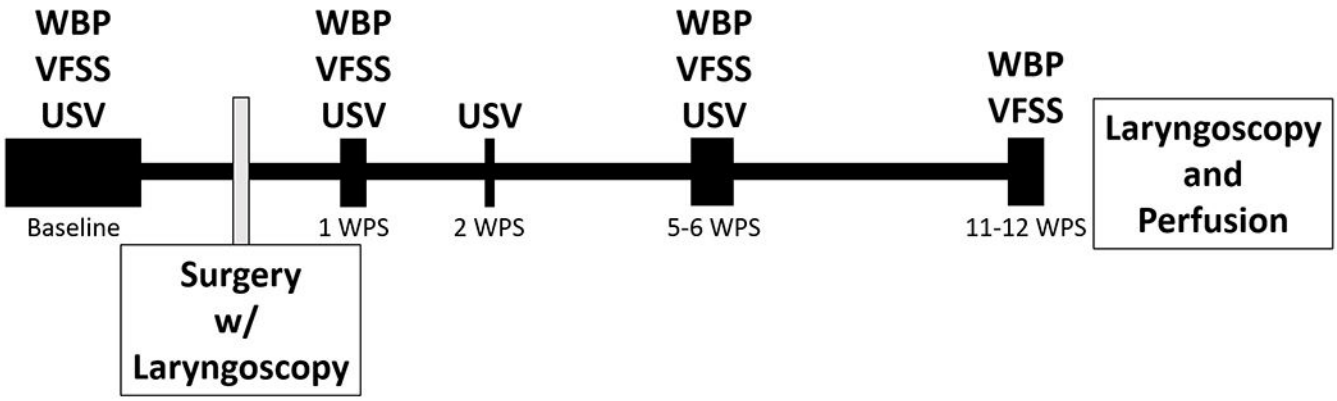

Figure 1.

Experimental Timeline. Baseline functional testing was performed 2-4 weeks prior to surgery. Additional functional analysis was performed following surgery. Whole body plethysmography was performed at 1,5, and 11 WPS. Videofluoroscopic swallow studies were performed 1, 6, and 12 WPS, and ultrasonic vocalizations were collected at 1,2, and 5 WPS. Laryngoscopy was performed prior to surgical incision, immediately following surgical manipulation of the RLN, and at 13 WPS prior to perfusion for tissue collection. WPS = Weeks post-surgery, WBP = whole body plethysmography, VFSS = videofluoroscopic swallow study, USV = ultrasonic vocalizations.

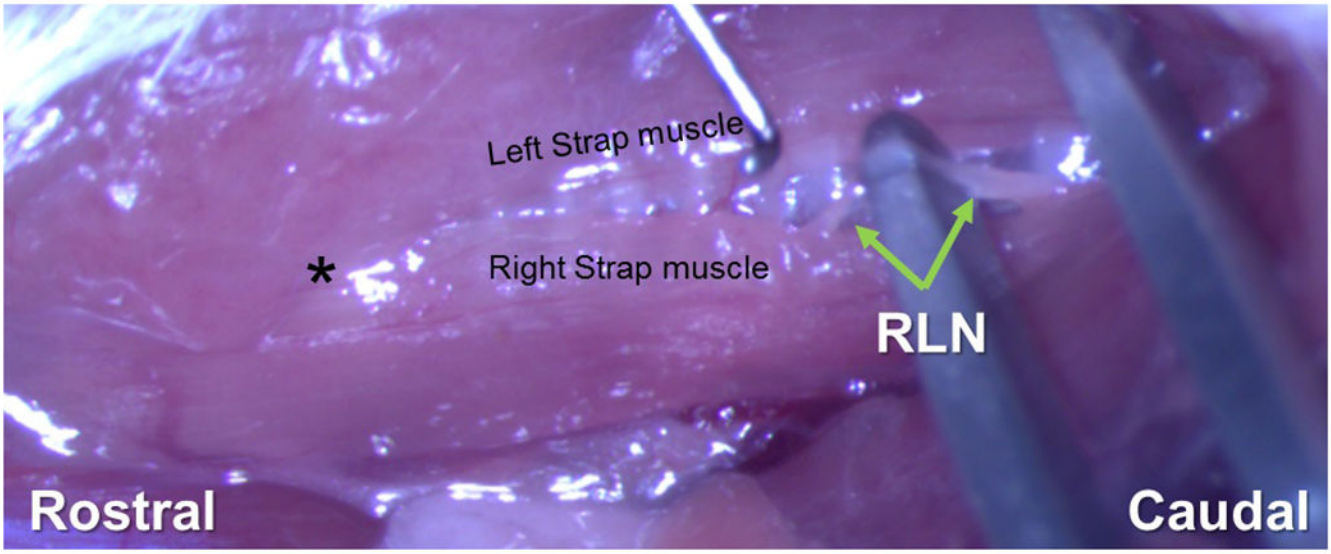

Figure 2.

Isolation of RLN Prior to Transection. The connective tissue between the left and right strap muscles overlaying the trachea is gently dissected. The right strap muscle is displaced laterally to identify the right RLN alongside the trachea. Here the right RLN is isolated and draped over a surgical tool prior to transection. The nerve is transected and 1-2 mm is removed near the 5th tracheal ring. * = region of the larynx

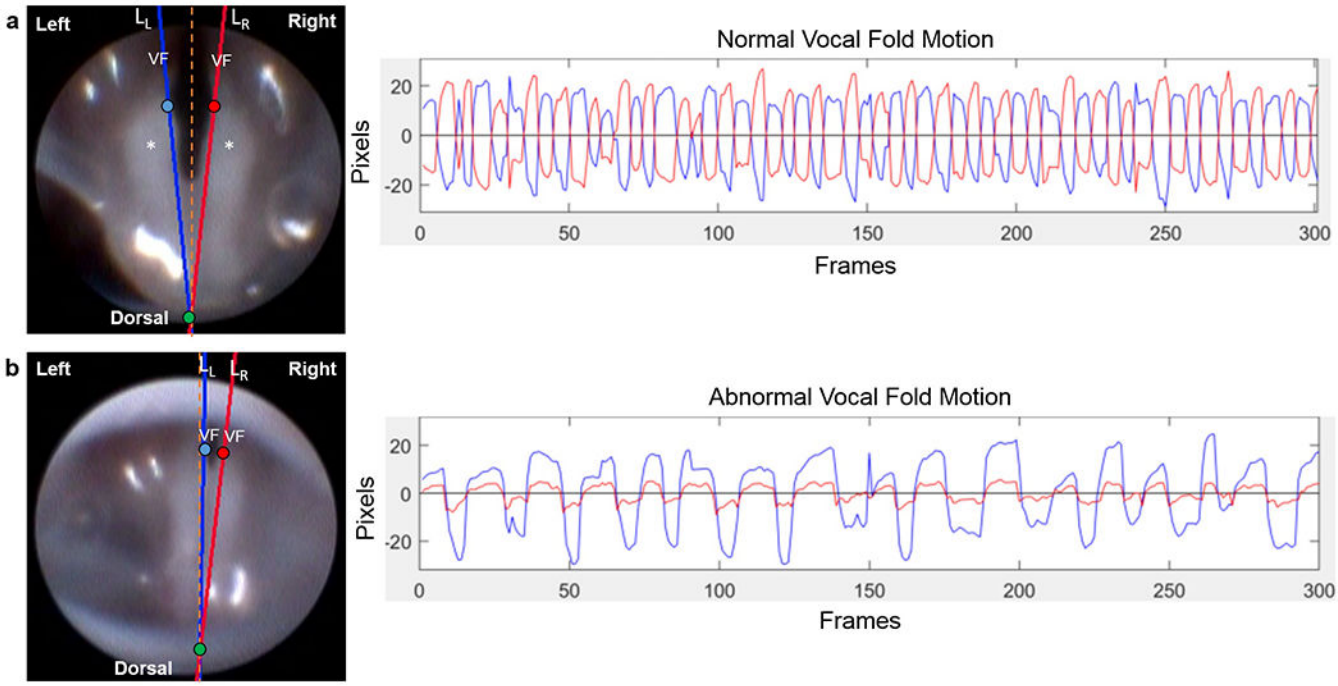

Figure 3.

Representative still frame images (left) and displacement plots (right) of normal versus abnormal (paradoxical) vocal fold motion. On the first frame of each endoscopic video clip, two points, p_L (blue circle) and p_R (red circle), were manually placed on the medial aspect of each VF and associated arytenoid cartilage, and a third point, p_o (green circle), was placed midline, dorsal to the arytenoid cartilages. Using these manual reference points, separate lines (L_L and L_R) were automatically drawn to approximate the medial edge of each VF/arytenoid for motion tracking analysis, after automatic adjustment to make points p_L and p_R at the same fixed distance from p_o. These still frame images represent the positioning of the VFs in a state of maximum adduction. Note the left and right VF are symmetrical and do not cross the glottal midline in normal VF motion (a). However, in abnormal cases (b), the left VF may cross the glottal midline and contact the right VF, pushing it laterally, such that both VFs are paradoxically moving in the same direction. Alternatively, the left VF may pull the right VF medially during abduction, resulting in a similarly positive correlated displacement plot. VF = vocal fold. Asterisk (*) = arytenoid cartilage. Orange dashed line = glottal midline. Plots show displacement of the intact left (blue) VF and denervated right (red) VF with respect to their motion midline (0 on y-axis) over time. Normal VF motion (a) is represented by oscillatory motion of both VFs in opposite directions (negatively correlated). Abnormal (paradoxical) VF motion (b) is represented by movement of the VFs in the same direction (positively correlated).

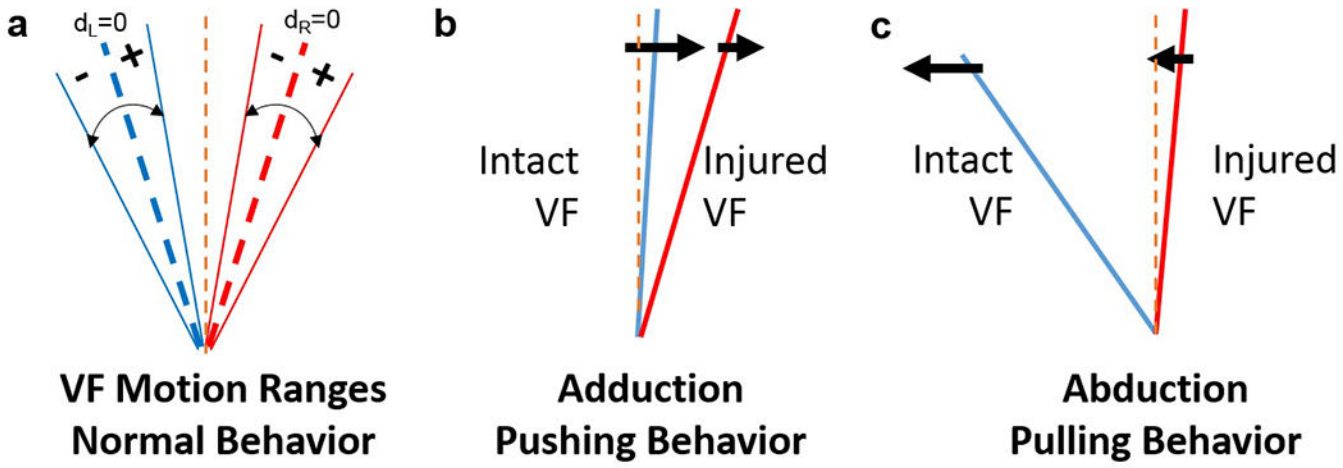

Figure 4.

Analysis of VF motion behavior. (a) Left and right VF motion ranges; center dashed blue and red lines represents motion midline for each VF (i.e., d_L= displacement of left VF = 0; d_R= displacement of right VF = 0). (b) VF motion during pushing: The intact VF contacts the injured VF to push it laterally in the same direction during VF adduction. (c) VF motion during pulling: The intact VF pulls the injured VF medially in the same direction during abduction. Left VF (blue line) represents the healthy, intact VF; right VF (red line) represents the injured VF. Orange dashed line = glottal midline.

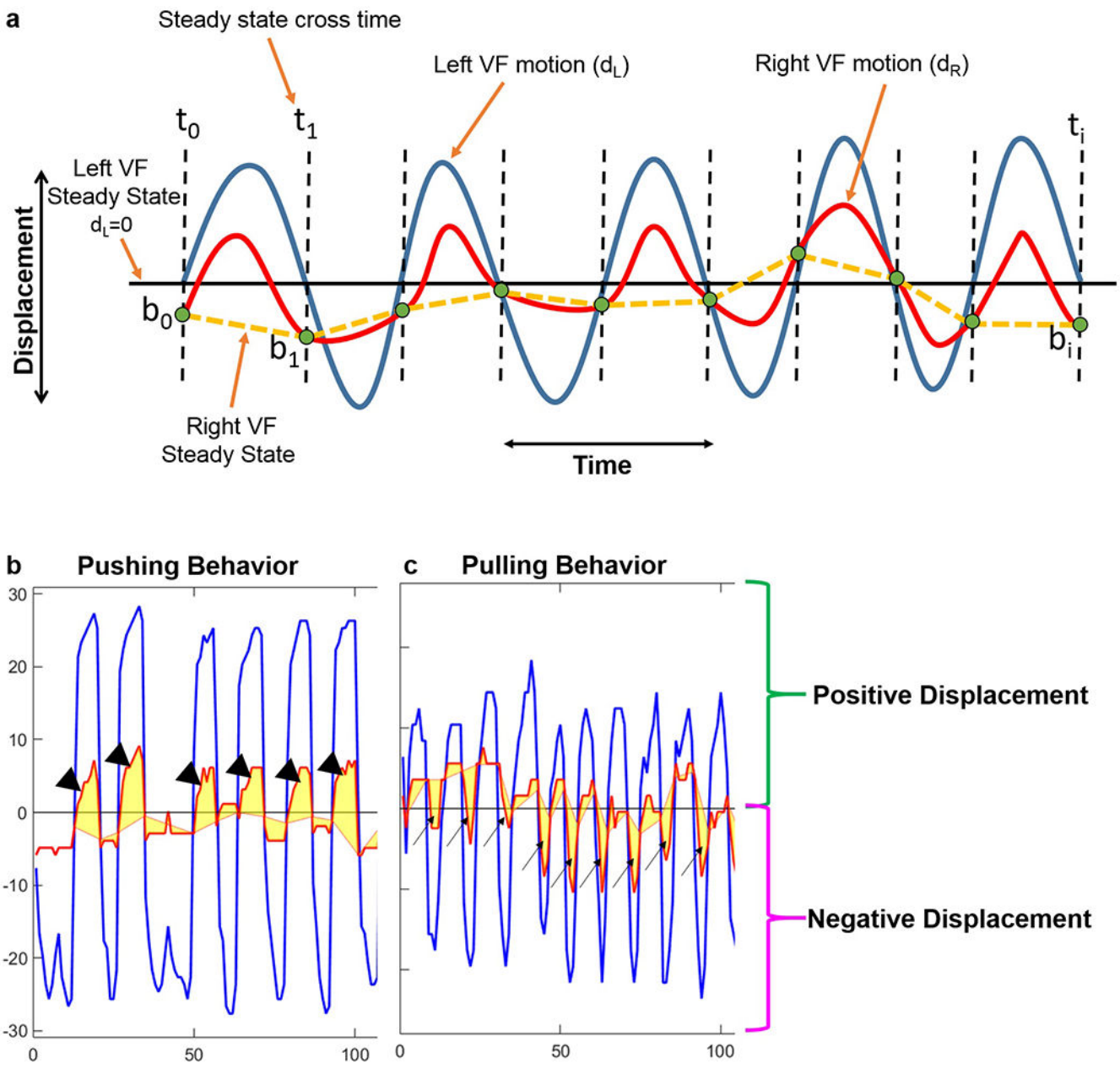

Figure 5.

Identification of pulling versus pushing behaviors from left and right VF displacement time series. (a) Synthetic plot illustrating analysis of pushing vs. pulling behaviors. Displacement of the left VF with respect to its motion midline is shown in blue. Displacement of the right VF with respect to its motion midline is shown in red. The solid black (horizontal) line illustrates the motion midline and steady state for the left VF. The dashed black (vertical) lines indicate where the left VF crosses its steady state position. The steady state position of the right VF is determined by the positions of the right VF when the left VF is positioned at its baseline (no pulling or pushing by the left VF). The dashed yellow lines denote the steady state positions for the right VF. Pulling versus pushing behaviors are identified by separately

computing total displacements of the right VF during positive and negative displacements of the left VF. (b) Representative plot for pushing behavior. Larger total absolute displacement by the right VF during positive displacements (arrowheads) of the left VF indicates pushing behavior. (c) Representative plot for pulling behavior. Larger total absolute displacement by the right VF during negative displacements (arrows) of the left VF indicates pulling behavior.

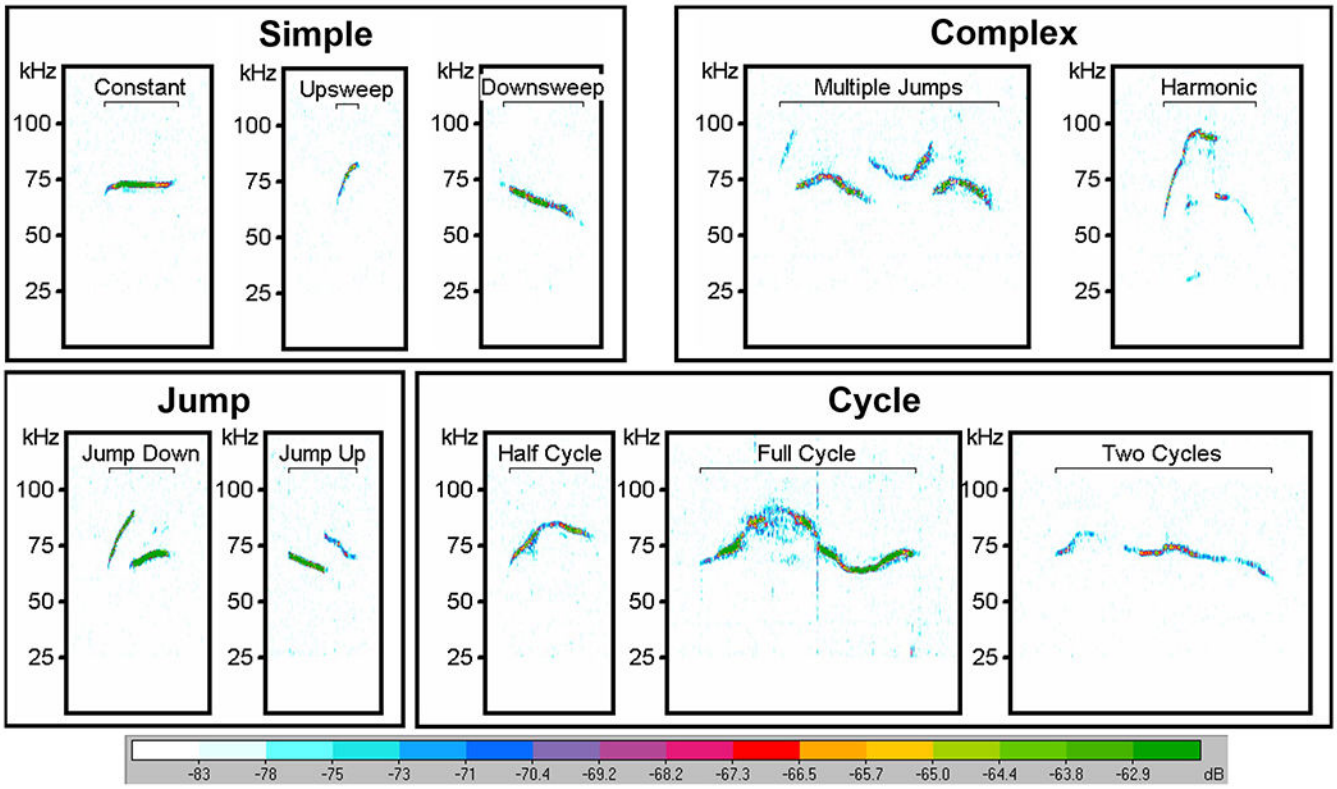

Figure 6.

Mouse USV Call Classifications. USV call types are classified into 4 call categories: simple, complex, jump, and cycle. Spectrograms are representative of baseline vocalization prior to any surgical manipulation. A high pass filter was used to eliminate noise below 25 kHz. Relative intensity ("vocal loudness") is measured in decibels (dB) and encoded by the color spectrum at the bottom of the image. The y-axis represents frequency of the call in kilohertz (kHz). USV = ultrasonic vocalization.

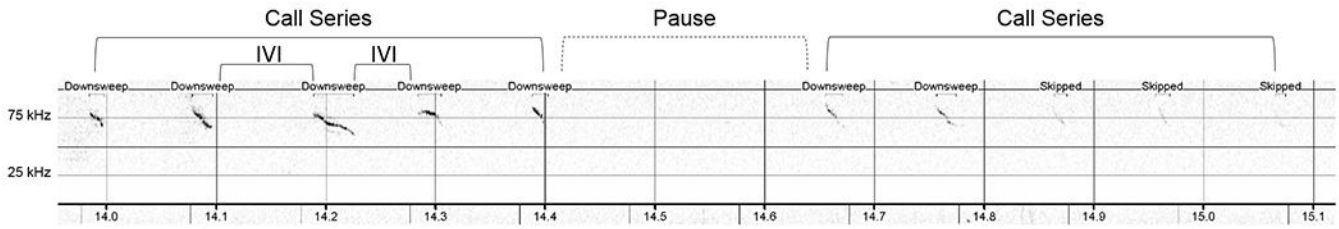

Figure 7.

Representative image of USV call runs and a pause. USV call series consisted of any group of calls with at least 4 calls spaced no more than 150 ms apart. Time between call series were considered pauses and may or may not have had isolated calls (groups of three or less calls) within the pause. The spectrogram X-axis represents time in seconds; the Y-axis is frequency in kilohertz (kHz). Relative intensity ("vocal loudness") is measured in decibels (dB) and encoded by darkness of the signal; louder is darker. Some calls were not automatically detected by the software. These calls were labeled as "skipped" but were included in call series if they were visually and audibly confirmed by the reviewer. IVI = Intervocalization Interval. USV = ultrasonic vocalizations.

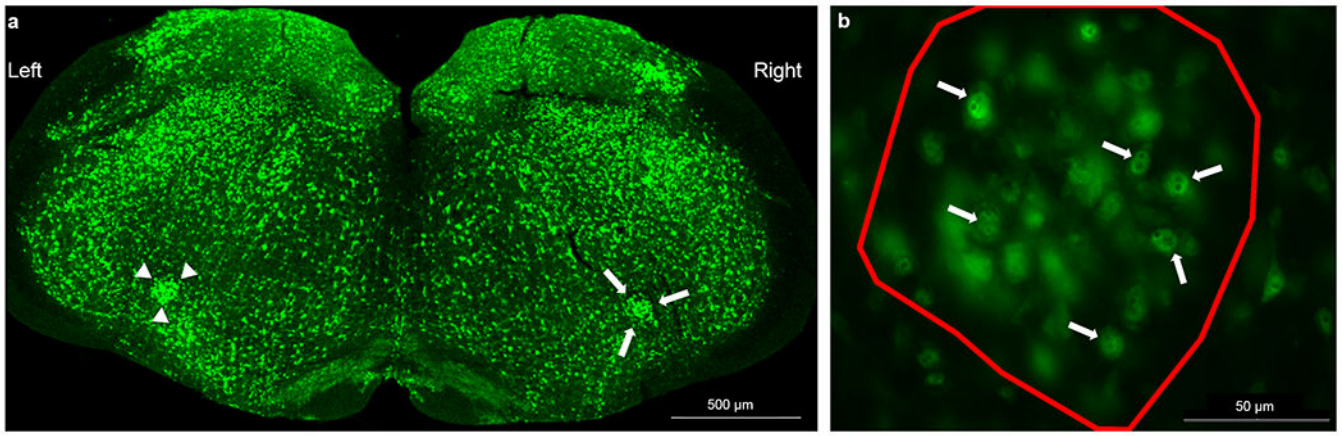

Figure 8.

Fluorescent immunohistochemistry of the nucleus ambiguus (NA). (a) 40 μm brainstem sections were stained with primary antibody (anti-NeuN; 1:500) followed by an Alexa Fluor 488-conjugated antibody (1:1000). Stereo Investigator software was used to outline the left (arrow heads) and right (arrows) NA with a 2.5x objective that permitted visualization of the entire brainstem section in a single field of view. (b) Neurons with a visible nucleolus (arrows) were counted for each NA (outlined in red) using a 40x objective throughout the entire 40 μm section.

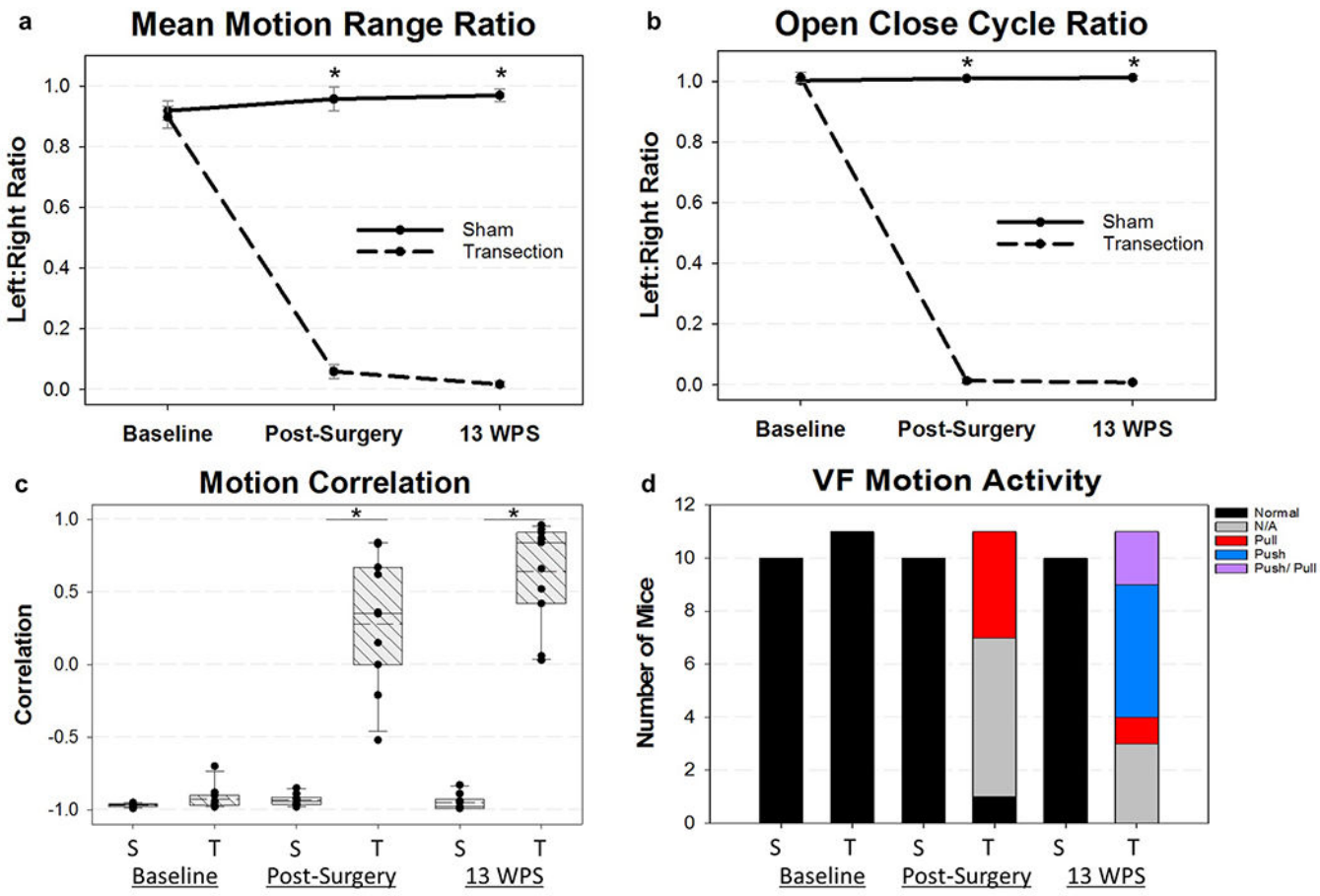

Figure 9.

Vocal Fold Motion Outcomes. (a) Mean Motion Range Ratio (MMRR) and (b) Open Close Cycle Ratio (OCCR) were significantly impaired in the RLN transected mice immediate post-surgery and at 13 weeks post-surgery (WPS). If mice were detected to have a positive cross correlation value (paradoxical movement), a 0 was assigned for MMRR. Additionally, the frequency threshold for OCCR was manually adjusted in our VFQuantify software to more accurately represent the true physiologic movement of the injured VF. (c) Vocal fold (VF) activity was assigned using a motion correlation coefficient (Mcorr) value. RLN transection resulted in mice with positive Mcorr values post-surgery and at 13 WPS. Median = solid horizontal line; Mean = dashed horizontal line. (d) VF motion activity was assigned as determined by the Mcorr value in combination with the left VF steady state motion. All mice at baseline had normal VF activity. However, mice undergoing RLN transection displayed abnormal pulling or pushing of the right VF by the left VF at the two post-surgical time points. At 13 WPS, 2 mice in the transection group had evidence of both pushing and pulling motion, and were manually assigned this dual classification. Mice with minimally correlative Mcorr values between −0.5 and 0.5 did not display normal VF motion nor the paradoxical pushing or pulling motion and received an activity classification of “N/A”. An asterisk (*) denotes statistical significance ($p < 0.001$). Error bars = standard error. S = Sham, T = Transection, WPS = Weeks Post Surgery, VF = Vocal Fold

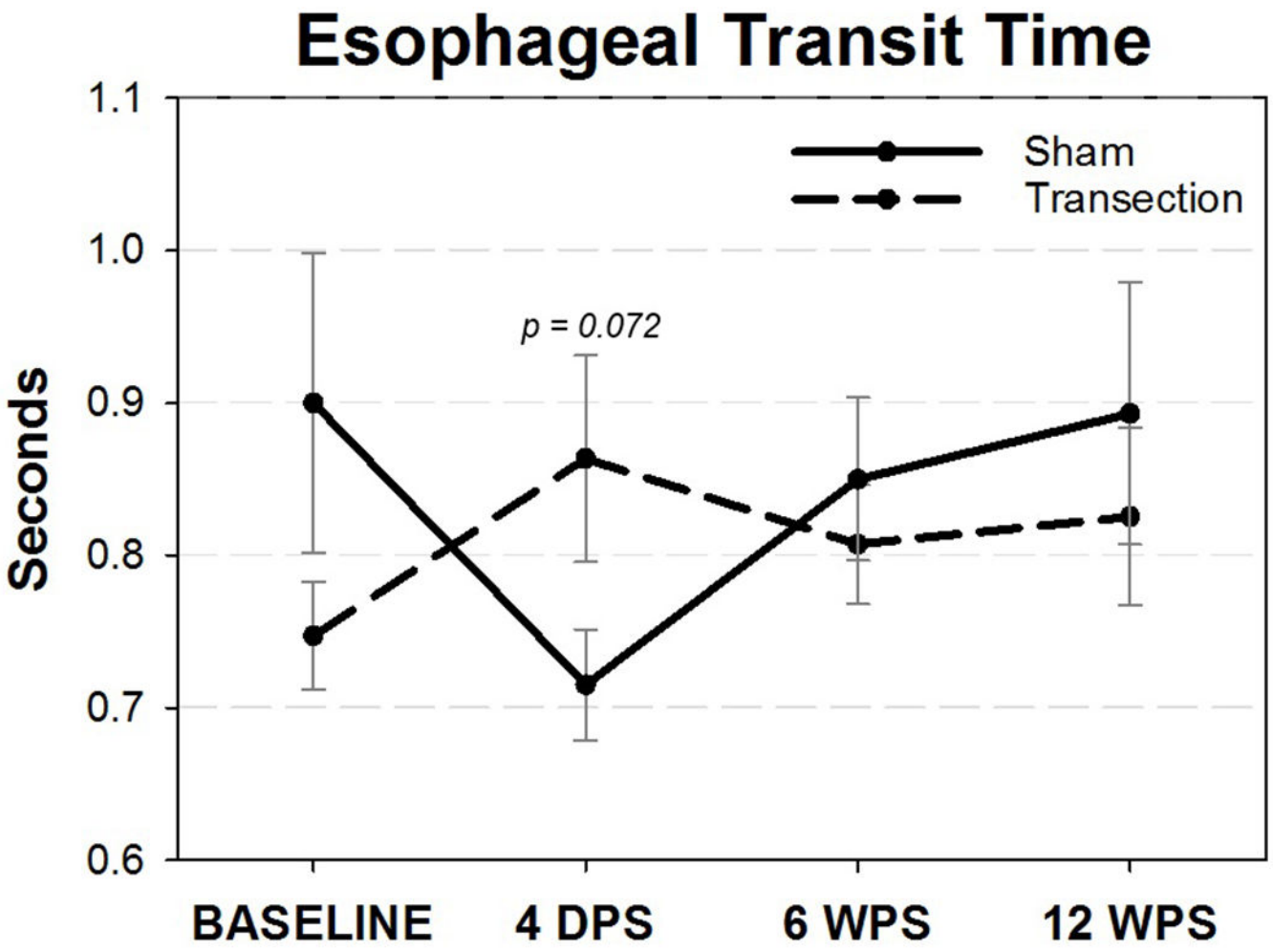

Figure 10.

Esophageal Transit Time (ETT). Though not statistically significant, mice in the RLN transection group had a trend for increased durations of ETT following surgery that appeared to recover by 6 WPS. On the other hand, sham mice had shortened ETT durations that also returned to baseline values by 6 WPS. WPS = Weeks Post-Surgery, Error bars = standard error.

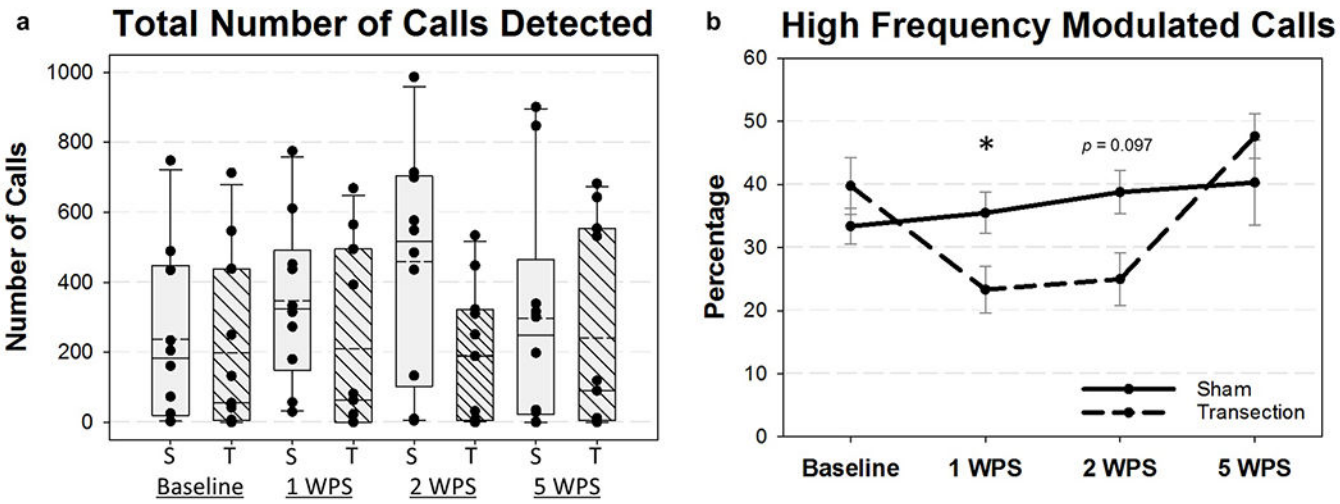

Figure 11.

Ultrasonic Vocalization (USV) Outcomes for all four time points. a) The total number of USV calls varied widely per group at each time point and were not significantly different between groups. Solid horizontal line = median; dashed horizontal line = mean; S = Sham, T = Transection. b) The percentage of high frequency modulated calls was significantly decreased in the RLN Transection group at 1 WPS, but recovered by 5 WPS. Only mice with greater than 20 calls were included in the analysis of high frequency modulated calls. WPS = Weeks Post-Surgery; S = Sham, T = Transection, Asterisk (*) = p = 0.031.

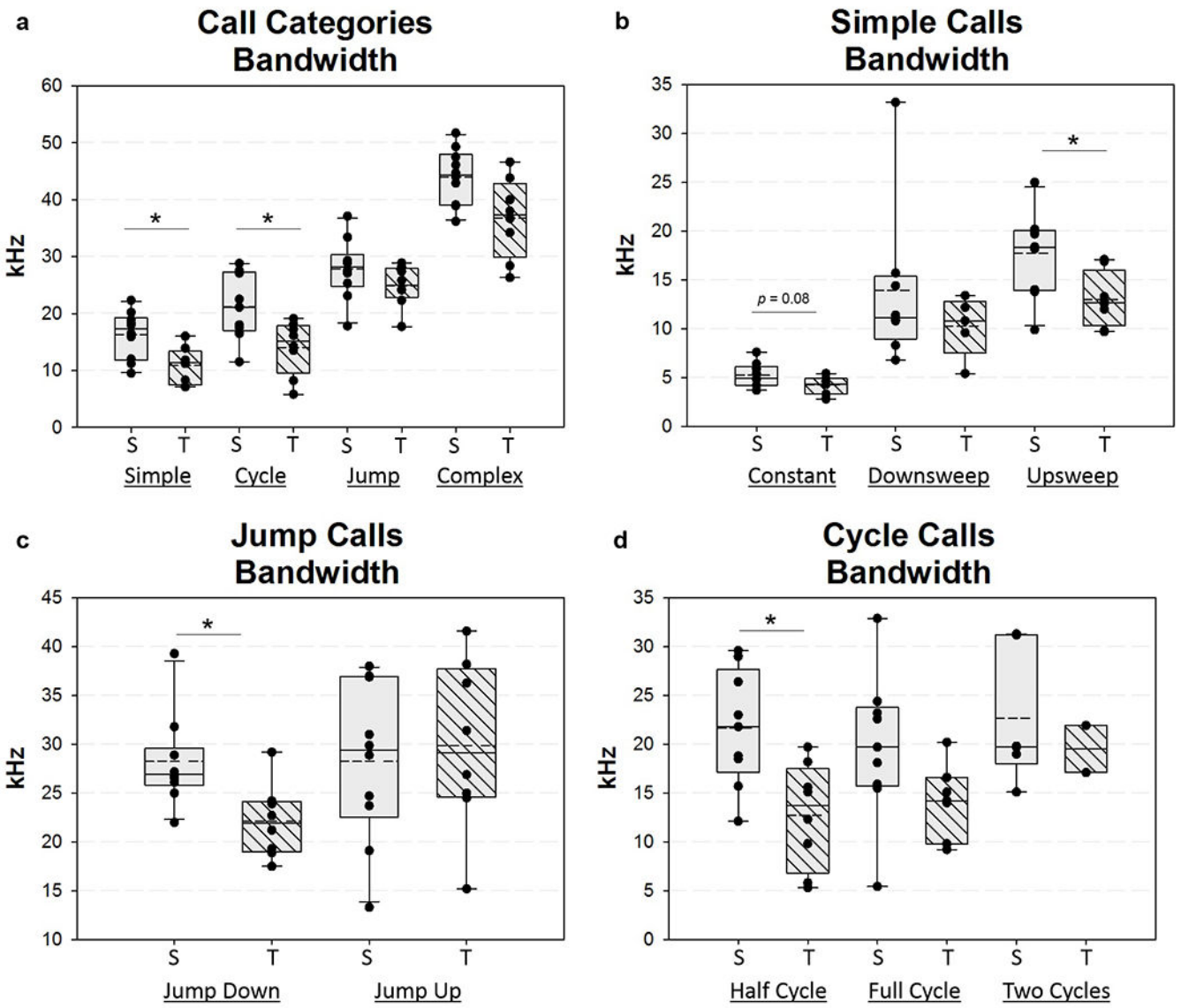

Figure 12.

Ultrasonic vocalization call bandwidth at 1 WPS. Box and whisker plots showing call bandwidth at 1 WPS for a) call categories, b) simple calls, c) jump calls, and d) cycle calls. Solid horizontal line = median, dashed horizontal line = mean, WPS = Weeks Post-Surgery; S = Sham, T = Transection, Asterisk (*) indicates significant difference between the two groups = $p < 0.05$

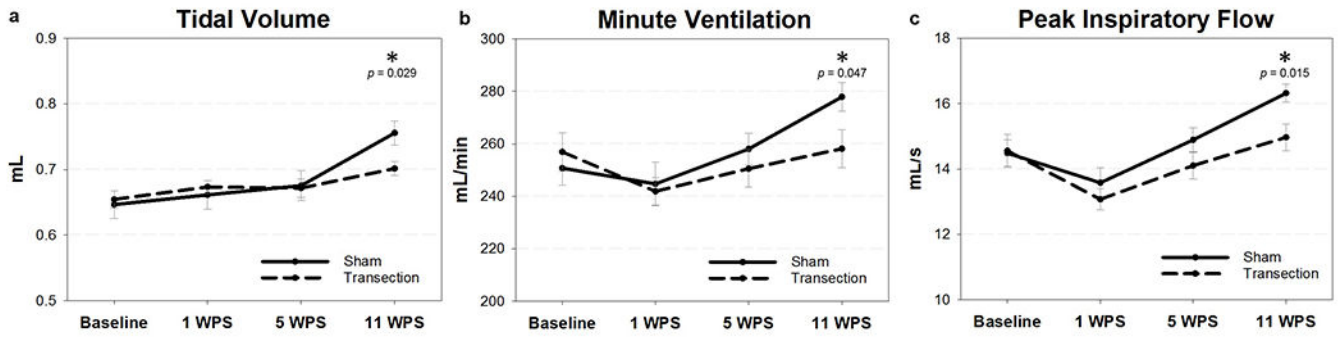

Figure 13.

Respiratory parameters during hypercapnic/hypoxic conditions. After normoxic conditions, mice were exposed to a hypercapnic (7% CO2)/hypoxic (10.5% O2) challenge to induce increased respiratory effort. There was a significant difference between groups at 11 WPS for (a) tidal volume, (b) minute ventilation, and (c) peak inspiratory flow. WPS = weeks post-surgery; mL = milliliters; s = seconds; * = significant p value ($p < 0.05$). Error bars = standard error.

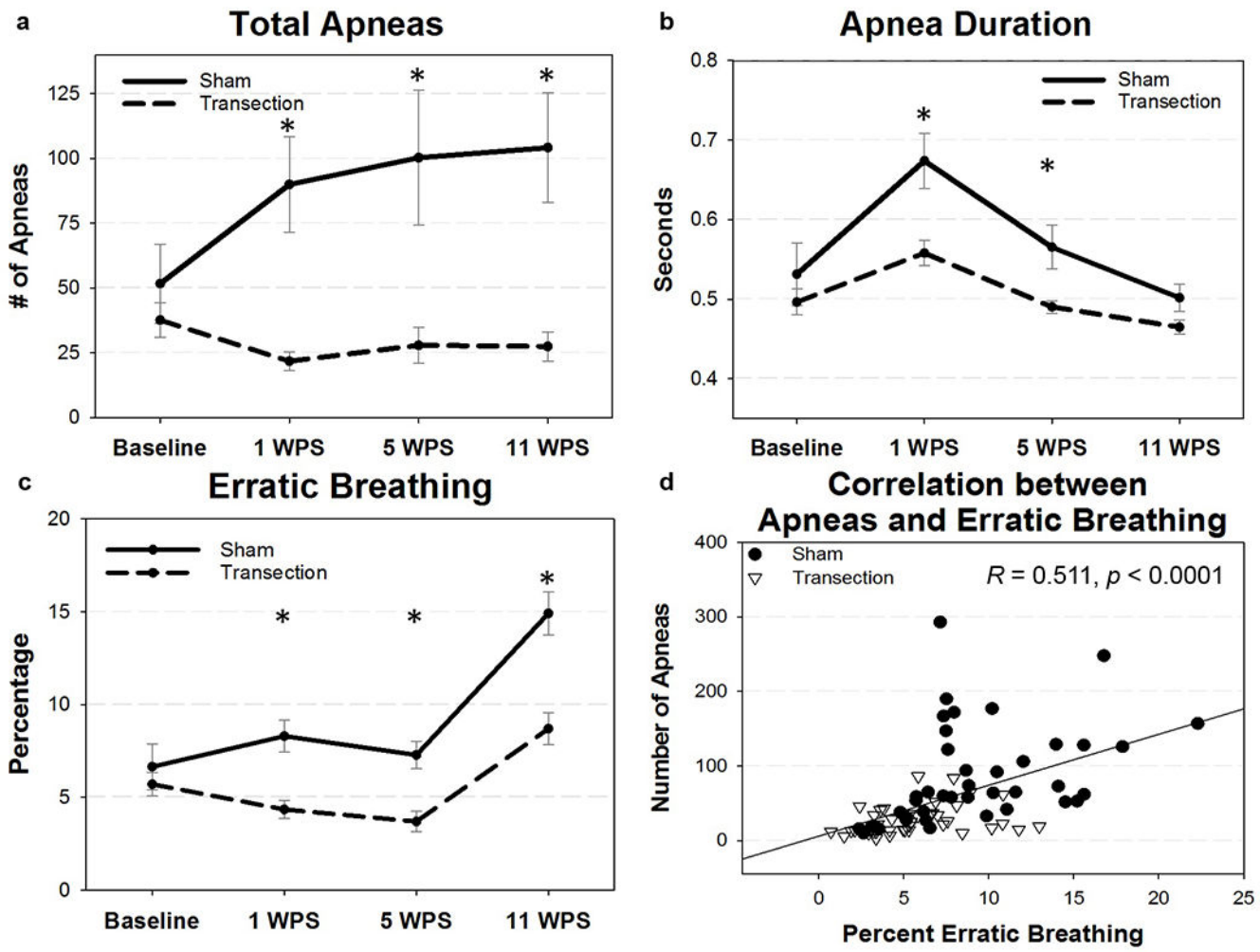

Figure 14.

Apnea respiratory outcomes, (a and c) RLN transection resulted in significantly less apneas and less erratic breathing in all three post-surgical type points. (b) Apnea duration significantly decreased in transected mice at 1 and 5 WPS as shown. (d) The number of apneas moderately correlated with the percentage of erratic breathing in both groups across all time points. WPS = weeks post-surgery; asterisk (*) denotes statistical significance with p values < 0.05. Error bars = standard error.

Table 1.

Experimental Methods

Hypothesis	Function Assessed	Methods Used	Time Points	Significant Outcome Metrics
H1	VF Movement	Transoral Laryngoscopy With Automated VF Tracking	Surgery: Pre-incision & Post-Transection 13 WPS	MMRR OCCR Mcorr
H2	Swallowing	Videofluoroscopic Swallow Study	Baseline 1 WPS 6WPS 12 WPS	n/a
H3	Vocalization	Ultrasonic Vocalization Assay	Baseline 1 WPS 2 WPS 5 WPS	High Frequency Modulated Calls Call Bandwidth ** Call Duration ** Intervocalization Interval
H4	Respiration	Whole Body Plethysmography	Baseline 1 WPS 2 WPS 11 WPS	Tidal Volume *** Minute Ventilation *** Peak Inspiratory Flow *** Apneas: Number & Duration Percent Erratic Breathing
H5	Neuronal Cell Counts *	Immunohistochemistry	13 WPS	n/a

Note: VF = Vocal Fold, WPS = Weeks Post-Surgery, MMRR = Mean Motion Range Ratio, OCCR = Open Close Cycle Ratio, Mcorr = Motion Correlation

* = Anatomical rather than functional assessment,

** = affected for a subset of call types,

*** = during respiratory challenge only

Table 2.

Videofluoroscopic Swallow Study Outcomes

VFSS Metrics units	Baseline		4 DPS		6 WPS		12 WPS	
	S	T	S	T	S	T	S	T
Lick Rate # per second	7.94 (0.60)	8.09 (0.30)	7.54 (0.57)	7.58 (0.42)	7.98 (0.55)	7.91 (0.50)	7.74 (0.43)	7.62 (0.56)
Swallow Rate # per 2 seconds	4.72 (0.70)	5.02 (0.60)	4.30 (0.76)	4.35 (0.59)	4.49 (0.86)	4.60 (0.61)	4.91 (0.56)	4.62 (0.40)
Inter-Swallow Interval seconds	0.48 (0.09)	0.42 (0.07)	0.53 (0.12)	0.53 (0.08)	0.54 (0.13)	0.49 (0.08)	0.45 (0.06)	0.46 (0.05)
Lick-Swallow Ratio Licks/swallow	3.08 (0.09)	2.75 (0.70)	3.42 (1.21)	3.40 (0.58)	3.76 (1.28)	3.22 (0.73)	2.80 (0.39)	2.80 (0.51)
Pharyngeal Transit Time seconds	0.10 (0.00)	0.10 (0.01)	0.11 (0.01)	0.11 (0.01)	0.11 (0.01)	0.11 (0.01)	0.11 (0.01)	0.11 (0.01)
Esophageal Transit Time seconds	0.90 (0.31)	0.75 (0.12)	0.71 (0.11)	0.86 (0.23)	0.85 (0.17)	0.81 (0.13)	0.89 (0.27)	0.83 (0.19)
Esophageal Swallow Inhibition percentage	36.0 (27.0)	22.0 (23.0)	8.0 (14.0)	15.0 (18.0)	32.0 (25.0)	27.0 (21.0)	32.0 (30.0)	25.0 (27.0)

Note: VFSS = Videofluoroscopic Swalow Study; S = Sham; T = Transection; DPS = Days Post-Surgery; WPS = Weeks Post-Surgery; VFSS metric values represent the mean (standard deviation).

Table 3.

Ultrasonic Vocalization Acoustic Parameter Outcomes

Percentage of Calls (%)										
Call Type	**Sham (n=10)**				**Transection (n=9)**				**F Value**	**P Value**
	Baseline		**1 WPS**		**Baseline**		**1 WPS**			
	$\bar{x}$	**SD**	$\bar{x}$	**SD**	$\bar{x}$	**SD**	$\bar{x}$	**SD**		
Simple	38.3	9.8	41.3	13.3	27.7	21.8	27.6	20.2	1.16	0.30
Constant	2.4	3.5	5.1	4.3	4.3	3.4	8.2	11.0	0.46	0.51
Downsweep	3.9	8.0	4.3	9.4	0.7	1.0	0.9	1.2	0.00	0.96
Upsweep	32.0	10.4	31.9	16.4	22.7	18.8	18.6	13.7	1.93	0.18
Jump	35.3	13.2	25.8	8.2	16.5	12.8	24.9	17.1	0.22	0.65
Jump Down	20.5	11.2	17.1	11.1	11.7	12.0	19.2	14.4	2.12	0.17
Jump Up	14.8	15.8	8.6	6.8	4.7	5.3	5.7	5.8	0.37	0.55
Cycle	8.3	7.7	11.4	6.7	12.8	9.2	7.8	7.0	1.45	0.25
Half Cycle	6.1	7.4	7.6	3.9	8.3	9.4	5.3	5.5	0.16	0.70
Full Cycle	1.8	2.2	3.2	2.7	4.2	4.2	2.3	2.2	0.42	0.53
Two Cycles	0.4	0.6	0.5	0.6	0.3	0.6	0.3	0.6	0.20	0.66
Complex	18.1	13.2	21.6	7.5	34.0	28.6	12.4	12.8	0.10	0.76
Multiple Jumps	14.1	11.7	14.2	6.5	29.3	28.7	12.0	12.6	3.74	0.08
Harmonic	3.9	3.4	7.3	4.7	4.6	7.4	0.4	0.7	17.79	**0.0007** *
Bandwidth (kHz)										
Call Type	**Sham (n=10)**				**Transection (n=9)**				**F Value**	**P Value**
	Baseline		**1 WPS**		**Baseline**		**1 WPS**			
	$\bar{x}$	**SD**	$\bar{x}$	**SD**	$\bar{x}$	**SD**	$\bar{x}$	**SD**		
Simple	17.9	3.7	16.3	4.2	17.9	5.6	10.9	3.2	10.94	**0.0048** *
Constant	6.9	3.8	5.2	1.2	6.2	1.8	4.2	0.9	3.90	0.08
Downsweep	18.1	10.5	13.9	8.3	11.5	5.5	10.3	3.1	1.46	0.28
Upsweep	18.0	3.9	17.7	4.2	20.0	5.2	13.0	2.8	11.48	**0.0041** *
Jump	25.1	8.0	27.9	5.3	27.7	3.8	24.8	3.7	0.45	0.51
Jump Down	26.3	2.9	28.2	4.7	26.7	3.2	22.1	3.7	6.40	**0.026** *
Jump Up	25.0	13.5	28.2	8.2	29.0	5.8	29.9	8.7	0.62	0.45
Cycle	23.4	8.1	21.2	5.9	19.6	7.1	14.0	4.8	4.94	**0.046** *
Half Cycle	20.7	5.5	21.7	6.0	19.0	6.1	12.7	5.4	6.41	**0.030** *
Full Cycle	23.9	8.3	19.7	7.5	18.6	7.3	14.1	3.8	3.39	0.10
Two Cycles	26.6	12.6	22.7	6.9	19.0	7.6	19.5	3.4	n/a	n/a
Complex	45.0	3.0	44.0	4.9	44.8	5.9	36.7	7.0	2.47	0.14
Multiple Jumps	42.8	5.2	43.7	4.1	44.0	6.7	36.8	6.9	2.83	0.12
Harmonic	47.6	6.8	42.5	13.3	45.6	7.5	39.8	13.8	0.07	0.80

Percentage of Calls (%)										
Call Type	Sham (n=10)				Transection (n=9)				F Value	P Value
	Baseline		1 WPS		Baseline		1 WPS			
	$\bar{x}$	SD	$\bar{x}$	SD	$\bar{x}$	SD	$\bar{x}$	SD		
Duration of Call (ms)										
Call Type	Sham (n=10)				Transection (n=9)				F Value	P Value
	Baseline		1 WPS		Baseline		1 WPS			
	$\bar{x}$	SD	$\bar{x}$	SD	$\bar{x}$	SD	$\bar{x}$	SD		
Simple	19.0	5.2	18.2	3.4	17.7	3.3	16.0	2.6	2.02	0.18
Constant	17.0	8.3	17.0	4.2	19.3	9.6	18.0	3.9	0.02	0.89
Downsweep	32.7	28.3	19.5	11.2	15.2	5.6	20.9	9.4	0.32	0.60
Upsweep	18.3	3.2	18.2	3.1	17.3	1.8	14.5	3.2	7.33	**0.016** *
Jump	26.5	11.1	29.0	7.1	34.5	10.1	27.7	8.0	0.16	0.70
Jump Down	27.5	4.7	28.2	7.8	35.0	7.3	27.0	7.7	0.08	0.79
Jump Up	20.5	8.5	29.4	7.4	30.3	14.3	27.0	7.7	0.33	0.58
Cycle	45.9	13.1	35.7	9.9	31.0	9.1	41.9	15.8	0.73	0.41
Half Cycle	38.5	10.0	29.9	7.5	27.8	7.5	35.1	15.6	0.75	0.41
Full Cycle	57.2	21.5	46.9	14.5	38.2	13.4	54.5	12.0	0.00	0.97
Two Cycles	70.4	35.8	72.3	31.9	60.8	45.9	127.3	25.7	n/a	n/a
Complex	47.5	9.3	50.5	15.6	50.3	15.8	59.7	14.7	1.15	0.31
Multiple Jumps	44.1	11.0	48.0	11.8	45.2	9.9	59.5	14.6	1.88	0.20
Harmonic	54.6	14.8	54.7	22.9	72.8	36.4	45.0	15.1	1.93	0.21
Peak Frequency of Call (kHz)										
Call Type	Sham (n=10)				Transection (n=9)				F Value	P Value
	Baseline		1 WPS		Baseline		1 WPS			
	$\bar{x}$	SD	$\bar{x}$	SD	$\bar{x}$	SD	$\bar{x}$	SD		
Simple	84.9	5.3	84.1	4.9	83.7	13.1	81.5	4.7	1.28	0.28
Constant	78.0	8.3	75.0	5.4	80.1	3.8	77.9	6.3	0.47	0.51
Downsweep	83.0	9.4	83.2	11.9	89.5	6.4	89.6	10.5	0.89	0.39
Upsweep	85.0	5.5	85.3	5.0	85.1	14.6	83.1	5.3	0.60	0.45
Jump	93.5	8.0	93.4	3.7	94.2	2.0	91.1	3.3	1.14	0.30
Jump Down	95.0	5.1	94.1	5.9	94.7	4.2	88.5	5.1	4.95	**0.046** *
Jump Up	93.0	11.0	93.7	7.6	95.9	7.4	94.5	8.4	0.40	0.54
Cycle	90.4	9.5	89.2	4.6	89.1	10.6	83.5	6.2	3.83	0.08
Half Cycle	88.7	6.4	91.0	6.1	91.2	15.1	83.0	8.2	3.72	0.08
Full Cycle	89.2	11.6	85.0	55.5	87.1	8.4	84.8	10.7	0.02	0.90
Two Cycles	89.3	9.4	82.7	7.8	87.2	9.6	84.7	4.2	n/a	n/a
Complex	107.3	3.1	106.7	2.2	105.8	7.5	99.9	7.4	3.82	0.07
Multiple Jumps	106.5	3.9	107.4	4.2	106.1	7.8	100.1	7.1	3.74	0.08
Harmonic	106.4	5.6	101.5	13.6	104.2	8.8	98.8	20.8	0.02	0.90

Percentage of Calls (%)										
Call Type	Sham (n=10)				Transection (n=9)				F Value	P Value
	Baseline		1 WPS		Baseline		1 WPS			
	$\bar{x}$	SD	$\bar{x}$	SD	$\bar{x}$	SD	$\bar{x}$	SD		
Duration of Peak Frequency (ms)										
Call Type	**Sham (n=10)**				**Transection (n=9)**				**F Value**	**P Value**
	Baseline		**1 WPS**		**Baseline**		**1 WPS**			
	$\bar{x}$	**SD**	$\bar{x}$	**SD**	$\bar{x}$	**SD**	$\bar{x}$	**SD**		
Simple	14.6	4.0	14.4	4.6	14.4	2.4	11.3	2.0	10.11	**0.0062** *
Constant	12.5	7.5	10.8	4.6	13.4	6.9	9.2	2.1	1.35	0.28
Downsweep	3.6	2.8	2.8	1.7	1.9	1.3	4.5	2.2	1.44	0.28
Upsweep	16.0	3.2	16.3	3.2	15.2	1.6	12.0	2.7	10.81	**0.005** *
Jump	13.9	2.5	14.5	4.4	17.8	11.0	11.6	3.0	1.72	0.21
Jump Down	11.8	4.1	11.3	4.7	12.7	2.7	8.7	3.1	0.80	0.39
Jump Up	16.5	5.4	20.5	5.4	21.5	11.1	18.5	4.1	0.10	0.76
Cycle	23.3	11.0	19.0	5.8	15.5	5.1	17.5	7.1	0.01	0.92
Half Cycle	23.6	10.8	16.8	4.7	14.8	2.8	13.6	5.5	0.33	0.58
Full Cycle	20.9	10.8	25.4	11.9	20.1	7.1	21.1	13.0	0.17	0.69
Two Cycles	18.0	14.5	35.3	30.1	16.2	5.4	46.6	33.8	n/a	n/a
Complex	21.1	5.1	21.4	4.0	21.6	4.1	23.8	8.0	0.71	0.42
Multiple Jumps	19.3	3.9	20.4	4.2	20.7	3.4	23.6	7.7	0.84	0.38
Harmonic	24.0	8.8	22.4	8.8	26.2	5.3	27.9	19.9	0.01	0.91

Note: $\bar{x}$ = mean; SD = standard deviation; WPS = weeks post-surgery; kHz = kilohertz; ms = milliseconds; bold values with an asterisk (*) = statistical significance ($p < 0.05$) between Sham and Transection groups at 1 WPS. Two mice from the transection group were excluded due to lack of calls. Outcomes could not be assessed for two cycle calls due to a very low percentage of mice with these types of calls.

Table 4.

Ultrasonic Vocalization Call Series Outcomes

USV Outcome Measure	Sham (n=10)				Transection (n=9)				F Value	P Value
	Baseline		1 WPS		Baseline		1 WPS			
	$\bar{x}$	SD	$\bar{x}$	SD	$\bar{x}$	SD	$\bar{x}$	SD		
Number of Total Call Series in 90 s	19.0	12.5	24.3	11.2	19.3	15.1	15.9	11.2	1.16	0.30
Number of Calls in a Series	10.5	4.3	11.4	3.7	9.7	2.3	9.3	2.5	0.84	0.38
Length of Series (s)	0.98	0.44	1.11	0.43	0.93	0.24	0.94	0.34	0.19	0.67
Longest Call Series (s)	3.58	4.71	5.55	4.73	3.14	1.96	3.52	3.20	0.75	0.40
Duration of IVI within a Series (ms)	74.5	8.7	71.1	6.5	71.4	5.3	82.0	10.1	7.20	**0.02** *
Pause Length (s)	4.33	4.26	2.83	2.59	3.65	3.06	4.52	3.67	0.43	0.52
Number of Calls in a Pause	2.69	1.69	3.11	1.38	3.32	1.55	6.21	3.73	3.37	0.09

Note: $\bar{x}$ = mean; SD = standard deviation; WPS = weeks post-surgery; IVI = intervocalization interval; s = seconds; ms = milliseconds; bold values with an asterisk (*) = statistical significance ($p < 0.05$) between Sham and Transection groups at 1 WPS. Two mice from the transection group were excluded due to lack of calls.

Table 5.

Normoxia Respiratory Outcomes

WBP Metrics units	Baseline		1 WPS		5 WPS		11 WPS	
	S	T	S	T	S	T	S	T
Frequency breaths/ minute	304 (44)	290 (44)	285 (67)	292 (68)	340 (44)	346 (42)	371 (23)	366 (28)
Tidal Volume ml	0.36 (0.07)	0.38 (0.05)	0.34 (0.06)	0.37 (0.03)	0.38 (0.06)	0.40 (0.04)	0.42 (0.06)	0.43 (0.03)
Inspiratory Time seconds	0.06 (0.01)	0.06 (0.01)	0.07 (0.02)	0.07 (0.01)	0.05 (0.01)	0.05 (0.01)	0.05 (0.00)	0.05 (0.01)
Expiratory Time seconds	0.16 (0.03)	0.18 (0.03)	0.18 (0.05)	0.18 (0.05)	0.15 (0.03)	0.15 (0.02)	0.13 (0.01)	0.13 (0.01)
Peak Inspiratory Flow ml/second	9.9 (1.7)	10.1 (1.8)	8.9 (2.6)	9.4 (2.1)	11.7 (2.3)	12.3 (1.9)	13.8 (2.6)	13.7 (1.5)
Minute Ventilation ml/ minute	106 (21)	109 (20)	96 (28)	105 (25)	131 (30)	140 (22)	155 (27)	155 (15)

Note: WBP = Whole Body Plethysmography; S = Sham; T = Transection; ml = milliliters; WPS = Weeks Post-Surgery; WBP metric values represent the mean (standard deviation).

Table 6.

Hypercapnia + Hypoxia Challenge Respiratory Outcomes

WBP Metrics units	Baseline		1 WPS		5 WPS		11 WPS	
	S	T	S	T	S	T	S	T
Frequency breaths/ minute	393 (38)	397 (39)	373 (33)	362 (33)	387 (33)	376 (39)	370 (22)	369 (24)
Tidal Volume ml	0.65 (0.07)	0.65 (0.04)	0.66 (0.07)	0.67 (0.03)	0.68 (0.07)	0.67 (0.05)	**0.76** * (0.06)	**0.70** * (0.04)
Inspiratory Time seconds	0.07 (0.01)	0.07 (0.01)	0.07 (0.01)	0.08 (0.01)	0.07 (0.01)	0.07 (0.01)	0.07 (0.00)	0.07 (0.01)
Expiratory Time seconds	0.09 (0.01)	0.09 (0.01)	0.09 (0.01)	0.09 (0.01)	0.09 (0.01)	0.09 (0.01)	0.09 (0.01)	0.09 (0.01)
Peak Inspiratory Flow ml/second	14.5 (1.3)	14.6 (1.6)	13.6 (1.4)	13.1 (1.1)	14.9 (1.2)	14.1 (1.4)	**16.3** * (0.09)	**15.0** * (1.4)
Minute Ventilation ml/ minute	251 (21)	257 (24)	245 (27)	242 (17)	258 (19)	251 (24)	**278** * (17)	**258** * (24)

Note: WBP = Whole Body Plethysmography; S = Sham; T = Transection; ml = milliliters; WPS = Weeks Post-Surgery; WBP metric values represent the mean (standard deviation). Bold values with an asterisk (*) denotes statistical significance ($p < 0.05$) between groups at the individual time point.